NASA-CR-201389

Report on the first year of NASA ADP grant NAG5-2999.

Grant Title:

Multiple Shells Around Wolf-Rayet Stars: Space-Based Astrometric Observing

PI:

Anthony P. Marston, Drake University

Introduction:

This is a report on the research progress made in the first year of a two year grant from the NASA ADP program (grant # NAG5-2999). This grant was awarded for the investigation of multiple shells around Wolf-Rayet stars. Primarily, the investigation was to involve the analysis of IRAS image data, particularly HIRES (high resolution) IRAS data, of the regions surrounding all galactic Wolf-Rayet stars. The intent of this investigation is to define parameters, such as time periods and mass-loss rates, associated with the multiple phases expected in the evolution of Wolf-Rayet stars. The use of the IRAS enables the cool gaseous material surrounding these stars to be visualized. Generally, only a portion of this gas can be seen in optical emission-lines and few Wolf-Rayet stars show large optical emission-line shells associated with their original O star progenitors.

Summary of Investigations:

In the past year the following work has been completed.

1. The completion of a complementary optical emission-line survey of the nebulae associated with Wolf-Rayet stars in the southern sky.
2. The completion of a survey the large-scale environments of Wolf-Rayet stars using IRAS Skyflux data.

3. The creation of HIRES IRAS maps in the four IRAS wavebands for approximately half of all galactic Wolf-Rayet stars (the rest are currently being created).

Summary of Data Analysis Results:

The results of two of the above investigations have been presented for publication. A presentation of the work undertaken with the aid of this grant was also made at the 187th American Astronomical Society (AAS) meeting in San Antonio, TX, 14-18 January, 1996. Copies of the two papers, "A Survey of Nebulae Around Galactic Wolf-Rayet Stars in the Southern Sky III. Survey Completion and Conclusions" by A. P. Marston (presented for publication in Astrophysical Journal Supplement) and "Large IRAS Shells Around Galactic Wolf-Rayet Stars and the O Star Phase of Wolf-Rayet Evolution" by A. P. Marston (presented for publication in the Astronomical Journal), are attached to this report. An abstract of the AAS meeting presentation is also attached.

Some of the main conclusions of these papers are:

1. Optical ring nebulae are consistent with the expected evolution of single (rather than binary) Wolf-Rayet stars.
2. Ring nebulae are consistent with a three phase evolution of Wolf-Rayet star from an O star progenitor, through a heavy mass-loss phase to the Wolf-Rayet phase.
3. The presence of wind-blown and ejecta shells appears to be independent of environment, suggesting such shells are primarily associated with the evolution of the Wolf-Rayet star and not with material accumulated from the local environment.
4. Large (>20') IRAS shells are seen around nearly a third of all Wolf-Rayet stars. These are also consistent with single, rather than binary, Wolf-Rayet star evolution, and appear to have been created by the sweeping up of the interstellar medium by the wind of the O star progenitor.
5. Time periods for the evolution of large IRAS shells are consistent with the predictions of the theory of single massive star evolution.
6. A possible trend exists between the mass of the progenitor to the O star and the local density of its surroundings.

Further investigations using HIRES data have shown the existence of previously unseen ejecta and wind-blown shells. An example is that of the nebula surrounding WR16 (see Fig. 1). The detailed morphology of many ejecta nebulae is now also available with HIRES data. Optical and HIRES data associated with the ring nebula(e) surrounding WR6 are currently being prepared for publication.

Publications:

The following are associated with this NASA grant.

Marston, A. P., & Yocum, D. R., 1996, BAAS, 27, 1345.
Marston, A. P., "A Survey of Nebulae Around Galactic Wolf-Rayet Stars in the Southern Sky III. Survey Completion and Conclusions", submitted to Astrophysical Journal Supplement.
Marston, A. P., "Large IRAS Shells Around Galactic Wolf-Rayet Stars and the O Star Phase of Wolf-Rayet Evolution", submitted to the Astronomical Journal.
Marston, A. P., "On the Origin of the Nebulae Surrounding the Wolf-Rayet Plus Compact Companion Candidate Star WR6", in preparation.

Future Investigations:

In the second year of the program we expect to have investigated HIRES data of regions associated with at least 90% of all known galactic Wolf-Rayet stars. These will provide particularly useful information regarding the ejecta rings surrounding many of these stars, including the likely lifetime of the mass-loss phase and total mass lost.

A small expansion to the program involves the investigation of mid- and far-infrared data associated with the Wolf-Rayet stars themselves in order to determine any evolutionary properties of the dust creation observed in near-infrared observations of the winds of these stars.

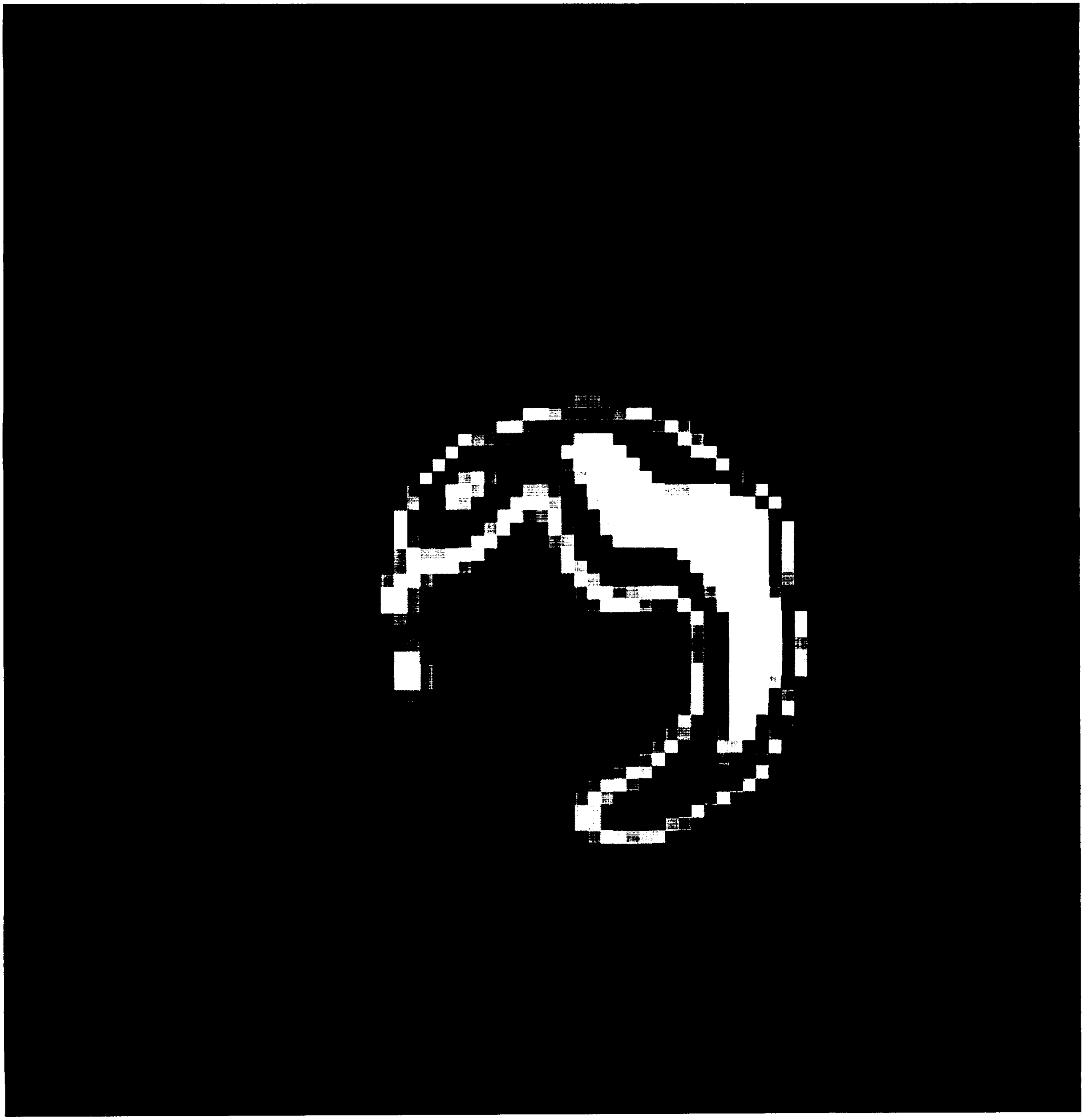

Fig. 1: The 60 micron HIRES IRAS image of the ring nebula around WR16. The field of view is 15'x15'.

Further Information:

For any further information regarding this project, please contact the principal investigator.

Tony Marston

A. P. Marston
Physics & Astronomy Dept.,
Drake University,
Des Moines, IA 50311,
USA
Tel: +1 515 271 3034   FAX: +1 515 271 3977
E-mail: tm9991r@acad.drake.edu

Abstract for poster at the 187th meeting of the American Astronomical Society, San Antonio, TX, 14-18 January, 1996.

IRAS Observations of Nebulae Around Wolf-Rayet Stars

A. P. Marston, Drake University, Des Moines, IA 50311.
&
D. R. Yocum, Kitt Peak National Observatory, NOAO, Tucson, AZ 85721.

Abstract:

We present IRAS Skyflux and high resolution (HIRES) images of the environments of galactic Wolf-Rayet stars. These form part of a complete sample of all galactic Wolf-Rayet stars observed by IRAS, a total of some 160 stars. The intent of this survey is to obtain information on the large bubbles expected from the early O star phase of Wolf-Rayet stars, as well as providing estimates of the dust and gas masses of any ejecta shells occurring after the O star phase, and seen interior to the O star bubbles. So far, a total of more than 40 probable or suspected shells of >20' in diameter have been observed in our data, which may be associated with Wolf-Rayet stars. We indicate how information from this work may be used to pin down parts of the evolutionary sequence of Wolf-Rayet stars, including estimates of the time periods for which both WN and WC subtypes spend in an O star and heavy wind stage.

A Survey of Nebulae Around Galactic Wolf-Rayet Stars in the Southern Sky III. Survey Completion and Conclusions.[1]

A. P. Marston

Dept. of Physics & Astronomy, Drake University, Des Moines, IA 50311

[1] Based on observations made using the Curtis Schmidt, CTIO. CTIO is operated by the Association of Universities for Research in Astronomy, Inc., under contract with the National Science Foundation.

Submitted to Astrophysical Journal Supplement.

Abstract

We present the conclusion of a narrow-band optical CCD survey of Wolf-Rayet stars in the southern portion of the Milky Way. In this part of the survey we complete our survey of the southern galaxy and report the detection of 10 new optical nebulae associated with Wolf-Rayet stars. This brings the final survey total to 40 Wolf-Rayet stars with associated nebulae in 114 southern galactic fields for a 35% detection rate. Our results suggest that the galactic environment has little apparent effect on the detection rate of nebulae associated with WR stars. Indeed, a more important role in the production of nebulae is likely to be played by the evolution of the central star. The survey results also suggest a slightly higher incidence of nebula detection around WN stars over WC stars, although nebulae associated with WC stars are noted as being generally larger and some may have been missed through being larger than the CCD array used. Indeed, the increased rate of nebula detection compared to that of a northern galaxy survey can be accounted for solely through the fact that a larger region of sky around the Wolf-Rayet stars was imaged in our southern survey as compared to the northern survey. Larger nebulae existing around WC as opposed to WN stars are also consistent with the current theory of the evolution of Wolf-Rayet stars f rom WN to WC.

1 Introduction:

Wolf-Rayet (WR) stars are believed to be the bare cores of evolved, massive stars. Stellar evolution models suggest that O stars of between 25 and 120 $M_\odot$ evolve to WR stars (Maeder & Meynet, 1994). The WR stars so formed are typically between 10 and 20 $M_\odot$, with the rest of their mass being ejected over the course of their lifetimes (e.g., Langer, 1990). Although WR stars presently lose significant mass in strong stellar winds, their current mass-loss rates are insufficient to account for the ejection of their former O star envelopes. Therefore, at some period in the past — perhaps during earlier red supergiant (RSG) and/or Luminous Blue Variable (LBV) phases (Humphreys, 1991; Kastner & Weintraub, 1995) — WR stars underwent phases of extreme mass-loss. If such is the case, then considerable amounts of circumstellar material is expected to exist around WR stars. In two previous papers (Marston *et al.*, 1994a, henceforth paper I; Marston *et al.*, 1994b, henceforth paper II) narrow-band optical imaging observations were presented of the environments of galactic WR stars in the southern sky. These illustrated that a considerable number of WR stars do indeed have associated, circumstellar emission-line nebulae. These observations suggested that circumstellar nebulae are almost ubiquitous. Indeed, a number of WR stars appear to have multiple, concentric nebular rings (paper II; Marston, 1995a; Dopita *et al.*, 1994). The existence of circumstellar material around WR stars, and particularly multiple concentric rings, enables indication of the evolution of these stars from study of their associated nebulae. A standard three-phase evolution of a massive O star through a heavy mass-loss stage to a WR phase is implied from optical and infrared observations (e.g. Marston, 1995a; Marston, 1995b).

In this paper we present the completion of our narrow-band optical survey of the environments of WR stars in the southern galaxy, and indicate the properties of the associated nebulae and factors affecting their detection. We also consider what circumstellar evidence exists for WR subtype evolution from WN to WC.

2 Observations:

The observations presented in this paper were made at the 24″ Curtis Schmidt telescope at Cerro Tololo Interamerican Observatory on the nights of 15 - 19 May, 1994. Observations were made using a 1024x1024 Thomson CCD chip, covering an approximately 31′x 31′ field of view, together with narrow-band filters centered on the optical Hα (6563Å, bandwidth 12Å) emission line. Typical integration times were 600 or 900 seconds. A table of the observations made for this final part of the survey is presented in Table 1.

3 Results:

In papers I and II a total of 30 of 88 WR stars in the southern galaxy were observed as having associated circumstellar nebulae. Here we present the results of imaging the final 26 southern galactic WR environments (plus WR99 was imaged but is no longer classified as a WR star, and WR 94 was reimaged due to dark count problems in earlier CCD imaging work). Of these, a total of 10 have evidence of associated circumstellar nebulae. Brief descriptions of new WR nebulae are presented below. Table 2 indicates the observed size and classification of the new nebulae. Classification is after Chu (1981), with W (wind-blown bubble from the WR phase), E (ejecta from a mass-loss phase) or R (radiative from the O star wind-blown bubble phase) nebular types.

3.1 WR20:

A partial outer ring (R; diameter of 43′) is observed to the north of this WN4.5 star (see Fig. 1). Some evidence of a continuation of the ring exists to the north west of the star.

3.2 WR20a/b:

These two stars, part of the Westerlund 2 open cluster are both of type WN7 (Shara *et al*, 1991). WR20a shows a blister type of morphology with part of the ring (of diameter 7.3′) having expanded out of the western edge of the cluster material (see Fig. 2). A ring also exists around WR20b with a diameter of 4.1′. The two rings appear to be colliding at the SE edge of the WR20a shell. The mass in the shells is likely to be associated with swept up, dense, gaseous material associated with the cluster and should be associated, primarily, with a slowly expanding bubble from the O star phase. The slow expansion deriving from a high ambient density. With such small O star progenitor bubbles, the ejecta material would easily fill them and the WR winds would, in turn sweep them out. In such a region of dense ambient gas, the nebulae associated with WR stars may well be material from each of the main evolutionary stages of the WR stars piled up on top of each other.

A larger ring arc is seen associated with the cluster towards the east which may well have been created by the combined effects of the stars in the cluster (see Fig. 3).

3.3 WR32:

This star resides in a cleared out region 27′ across, which is likely to have been formed during the O star, progenitor, phase of the WR star (see Fig. 4). This new shell is of R type.

3.4 WR35:

New ring of type R (see Fig. 5) approximately 25′ across, most likely associated with the O star phase. Nebulosity also appears to exist around the central star which is of type WN6. This nebulosity may well be associated with an apparently small ejecta shell of material. This star is placed at a distance of 16kpc by Conti & Vacca (1990) and the outer shell therefore has a physical diameter of 117pc. Shells of this size have been noted before as HI holes in the interstellar medium surrounding WR stars (Cappa de Nicolau & Niemela, 1984; Dubner *et al.*, 1990; Arnal, 1992; also see Marston, 1995b, and references therein).

3.5 WR35a:

A large, lopsided bubble is observed around this WN6 star (Shara *et al.* (1991). The WR star is 8300pc away, so the physical size of the observed bubble is 25pc (see Fig. 6). This shell would also appear to be of R type and is likely to have been produced in the O star progenitor stage of WR evolution.

3.6 WR35b:

A possible new shell is associated with this WN4 star. Strong nebulosity is noted 10′ north of the star and a fainter shell is evident to the west. The star resides in an open cluster and it is possible that the combined stellar winds from the cluster were responsible for the creation of this partial ring (see

Fig. 7).

3.7 WR36:

Definite new ring (see Fig. 8) with some similarities to that around WR35b. Here, the shell is complete, although much stronger to the eastern edge. It appears likely that the strong nebulosity to the east marks the boundary of two colliding shells or a collision of the WR shell with a region of enhanced density. The existence of the central WN4 star closer to the eastern edge suggests that the nebular expansion has indeed been curtailed in this direction. The nebula appears to be of R type.

3.8 WR42d:

A small, cleared region 2.5′ across is observed around this star, which is close to the large HII region NGC3603 (see Fig. 9). This may be associated with an ejecta (E) shell or a W/E shell, where a wind is penetrating a region of ejecta. The higher density of material in close to NGC3603 (evidenced by the surrounding diffuse emission) may have hindered the nebular expansion. At a distance of 2.8kpc (Shara *et al.*, 1991) this nebula is 2pc across.

3.9 WR94:

A weak shell approximately 11′ across is observed around this WN6 star (see Fig. 10). The weak, nebulous filling of the ring suggests it is likely to be associated with an ejecta (E) phase of the evolution of the central WR star. This region was observed for paper II when no associated nebula was seen. However, dark count problems existed for these earlier observations.

4 Combined Survey Results:

A synopsis of the results for observed nebulae in the complete southern survey is presented in Table 2, including estimates of nebular radii based on the distance measurements of Conti & Vacca (1990). In total 40 nebulae were observed as having apparent associations with WR stars, out of 114 environments, providing a detection rate of 35%. One nebula exists around 3 WR stars and a second one exists around a pair of WR stars, removing these still provides a detection rate of 35% for "single" WR stars.

There are numerous factors that might affect the detection of ring nebulae around WR stars.

a) intrinsic brightness/intensity of emission.
b) distance and absorption.
c) size relative to the size of the detector.

In considering galactic latitude (b), the detection rates change so that stars observed more than 2° above or below the galactic plane have a 32% chance of an associated nebula, while those at a galactic latitude of less than 1° have a 40% detection rate (see Fig. 12).

In the creation of R type ring nebulae. The lower ambient density associated with shells appearing higher above the galactic plane might be expected to lead to larger and intrinsically lower brightness, progenitor O star shells. However, such shells are expected to be generally less easily confused with other nebulae in the line of sight than those in the galactic plane. Some objects are formed in regions of higher density where the O star progenitor wind may be unable to create a large cavity and so can have ejecta and WR wind-blown material superimposed on the O star shell (e.g. WR20a/b). Such objects would not necessarily be observed as of R type, however. Overall, only a small difference in the detection rate of R type nebulae is noted, when comparing objects with b<2° and b>2° (9% as compared to 7% of observed WR stars). This is in direct contrast to the results of IRAS studies (Marston & Yocum,1996; Marston, in preparation), where the likelihood of an IRAS shell >20′ across was observed to increase sharply with galactic latitude. The IRAS shells are most likely to be associated with the optical R type shells. The IRAS results would therefore indicate that, generally, R type shells at higher galactic latitudes are physically larger (due to expansion into low ambient densities) and appear larger on the sky. Their detection rate is therefore affected by the fact that they are generally too large for the optical CCD array and have weaker optical emission-line intensity due to their distance from the central WR star. Also, WR stars of high galactic latitude are generally closer, once again leading to a tendency for R type rings too large for the CCD array used. This offsets the confusion in the galactic plane which reduces the R type ring detection rate for galactic latitudes of b<1°.

For W and E type shells, their detection is expected to be a function of evolution rather than environment, since the region into which these shells are moving has been swept out during the earlier O star phase. It might be expected that line-of-sight confusion would cause some difference in the detection rates of such nebulae with galactic latitude. Some reduction in their detection rate might be expected in the galactic plane as compared to away from the plane. Of the W and E type nebulae, 25% of those stars with b>2° have associated W or E type nebulae as compared to 27% of those with b<2°. The result suggests little differences in W and E type ring detection rates with environment.

5 Discussion:

Our southern galaxy survey indicates that nebulae surrounding WR stars are very common, and have so far been observed associated with just over one third of all southern galaxy WR stars. Results could be combined with the northern survey of Miller & Chu (1993), however, the northern survey was performed with an array having only a 15′ field of view. This restriction affects the detection rate of associated nebulae in the northern hemisphere. If we restrict the southern survey to rings of diameter <20′ then a detection rate of only 23% would have been noted, which is more consistent with a rate of 21% from Miller & Chu (1993).

Overall, the variation of environment with galactic latitude would appear to have only a limited effect on W/E ring detection rate. These results suggest that the galactic environment of WR stars does not play a major part in the creation of optically observed ring nebulae. Further, since most optically observed ring nebulae are of the wind-blown bubble (W) or ejecta (E) type, the unvarying detection rate with galactic latitude is consistent with material in these nebulae being predominantly composed of ejecta or swept-up ejecta from the WR stars, rather than the local interstellar medium, a result which has been suggested from studies of the chemical composition of WR ring nebulae (e.g. Chu, 1990; Esteban *et al.*, 1992). The detection of W and E type nebulae would then be solely dependent on the evolution of the WR star. Indeed, this can be turned around to indicate that the nebular environment of WR stars can be used to probe their evolution (Marston, 1995a).

According to the theory of the evolution of single WR stars (e.g. Maeder & Meynet, 1994), it is expected that WN stars will evolve to become WC stars. The wind-blown bubbles (W) produced in the WR stage would then be expected to be, generally, larger for those stars that have evolved on from WN to WC subtype. A comparison between the distributions of observed ring sizes for WN and WC type stars is shown in Fig. 12. From this we can see that only 4 out of 50 WC stars (36% of W/E nebulae observed around WC stars) have associated W/E nebulae with diameters of 10pc or less, while 11 out of 59 WN stars (65% of W/E nebulae observed around WN stars) have associated W/E nebulae of such sizes. Our results are in general agreement with a WN to WC subclass evolution, with larger nebulae existing around the older, WC type, stars.

In considering the WN and WC subclassifications, nebulae associated with the WN stars were observed 39% of the time while those associated with WC stars were observed 32% of the time. One possible reason for the slight increase in the detectability of nebulae associated with WN stars may the interaction between the mass-loss, ejecta shell and the WR wind-blown bubble of material, which is most likely to occur in the WN phase of the star. As the WR wind drives material into and through an ejecta shell, large-scale cooling should occur and the nebula brightens making it more easily detectable. An estimate of the period of time the star would need to be in the WR phase before this happens can be estimated following the arguments of Marston (1995a). We take the WR wind-blown bubble as expanding at a constant rate, v_{WR}, in ejecta with an r^{-2} distribution, and the ejecta as expanding at a constant rate, v_{ML}, from the start of a mass-loss phase. Therefore the time before the interaction, t_{int}, of these two shells is

$$t_{int} = \frac{v_{ML}.t_{ML}}{(v_{WR} - v_{ML})} \tag{1}$$

where t_{ML} is the period of the mass-loss phase. Assuming the mass-loss phase to be a LBV, a typical value of t_{ML} is 4×10^4yrs (de Koter, 1993). Taking a typical expansion velocity for a LBV nebula, v_{ML}, to be 50kms^{-1} (e.g. Nota *et al.*, 1995) and that of a WR shell to be 85kms^{-1} (as is the case for NGC6888, Marston & Meaburn, 1988), we obtain a period of approximately 6×10^4yrs. This is shorter than the average time required for a star to evolve from WN to WC subtype (Maeder & Meynet, 1994). An interaction between a wind-blown bubble and an ejecta shell would therefore occur during the WN phase.

6 Conclusions:

We have presented the final part of our survey of the environments of WR stars in the southern galaxy. Our observations have revealed a further 10 nebulae associated with WR stars. Survey results have shown that just over one third of all WR stars have associated nebulae which can be observed through optical narrow-band imaging. This is a higher percentage than that found by Miller & Chu (1993) in their survey of northern galactic WR stars, which is most likely to be due to the restricted field of view (15′x 15′) used in the northern survey. Restricting the southern survey to this size provides a detection rate of 23%, similar to that of the northern survey results of Miller & Chu (1993). Two stars in our survey have previously been noted as having associated nebulae which are larger than our CCD array and were therefore presented in our survey as having no associated nebulae detected, these are WR53 (associated nebula is RCW78) which has a diameter of 39′ , and WR48 (θ Mus) which has a diameter of 85′x40′ (Lozinskaya, 1992).

Our results are consistent with a general evolution that has WR stars progressing from O star progenitors, through a heavy mass-loss phase to a WR phase. They are also consistent with an evolutionary sequence from WN to WC subtypes, as nebulae around WC stars are generally larger than those surrounding WN stars. The difference in nebula size has made nebulae around WN star more detectable in earlier work on ring nebulae with smaller CCD arrays, suggesting a preference towards nebulae associated with WN over WC stars. This preference exists in our data but is not very strong. Some enhancement in nebular detectability might be expected from the interaction of a WR wind-blown bubble with an ejecta shell, which would be expected to occur predominantly in the WN phase of a WR star, prior to it becoming a WC star.

The galactic environment appears to have little effect in the optical detection of associated nebulae. The most likely reason for this is that most observed optical nebulae are associated with the mass-loss and WR phases of the star. If the materials in such nebulae predominantly come from the central star, then the evolution of the central star rather than the stellar environment plays the most important role in supplying the material for the nebula and therefore in the likelihood of the detection of an associated nebula.

APM acknowledges the support of the NASA JOVE grant NAG8-264 and NASA ADP grant NAG5-2999. APM would like to thank Dan Yocum for assistance at the telescope.

REFERENCES

Arnal, E. M., 1992, A&A, **254**, 305.

Cappa de Nicolau, C., & Niemela, V. S., 1984, AJ, **89**, 1398.

Chu, Y.-H., 1981, ApJ, **249**, 195.

Chu, Y.-H., 1990, In IAU Symp. 143, Wolf-Rayet Stars and Interrelations with Other Massive Stars in Galaxies, ed. K. A. van der Hucht & B. Hiddayat (Dordrecht: Kluwer), p.349.

Conti, P. S., & Vacca, W. D., 1990, AJ, **100**, 431.

Danks, A. C., Dennefeld, M., Wamsteker, W., & Shaver, P. A., 1983, A&A, **118**, 301.

Dopita, M. A., Bell, J. F., Chu, Y.-H., & Lozinskaya, T. A., 1994, ApJS, **93**, 455.

Dubner, G. M., Niemela, V. S., & Purton, C. R., 1990, AJ, **99**, 857.

Esteban, C., Vilchez, J. M., Smith, L. J., & Clegg, R. E. S., 1992, A&A, **259**, 629.

van der Hucht, K. A., Conti, P. S., Lundstrom, I., & Stenholm, B., 1981, Space Sci.Rev., **28**, 227.

Humphreys, R. M., 1991, In IAU Symp. 143, Wolf-Rayet Stars and Interrelations with Other Massive Stars in Galaxies, ed. K. A. van der Hucht & B. Hiddayat (Dordrecht: Kluwer), p.485.

Kastner, J. H., & Weintraub, D. A., 1995, ApJ, **452**, 833.

de Koter, A., 1993, Ph.D. thesis, Univ. of Utrecht.

Langer, N., 1990, A&A, **248**, 531.

Lozinskaya, T. A., 1992, in *Supernovae and Stellar Wind in the Interstellar Medium*, AIP, New York, p. 321.

Maeder, A., & Meynet, A., 1994, A&A, **287**, 803.

Marston, A. P., & Meaburn, J., 1988, MNRAS, **235**, 391.

Marston, A. P., Chu, Y.-H., & Garcia-Segura, G., 1994a, ApJS, **93**, 229. (paper I)

Marston, A. P., Yocum, D. R., Garcia-Segura, G. S., & Chu, Y.-H., 1994b, ApJS, **95**, 151. (paper II)

Marston, A. P., 1995a, AJ, **109**, 1839.

Marston, A. P., 1995b, AJ, **109**, 2257.

Marston, A. P., & Yocum, D. R., 1996, BAAS, **27**, 1345.

Miller, G., & Chu, Y.-H., 1993, ApJS, **85**, 137.

Niemela, V. S., & Cappa de Nicolau, C. E., AJ, 101, 572.

Nota, A., Livio, M., Clampin, M., & Schulte-Ladbeck, R., 1995, ApJ, **448**, 788.

Shara, M. M., Moffat, A. F. J., Smith, L. F. & Potter, M., 1991, AJ, **102**, 716.

Table 1: Final set of narrow-band imaging observations, completing the southern survey of WR environments.

WR #	WR type	Integration time	Figure	Comments
19a[1]	WN7	900		
20	WN4.5	900	1	new, large ring
20a[1]	WN7	900	2&3	blister nebula associated with cluster
20b[1]	WN7	900	2&3	close to 20a
30a[1]	WC4+O4	900		diffuse emission to N&S
31a[1]	WC6	900		in diffuse emission
32	WC5	900	4	large cleared region
33	WC5	900		
34	WN4.5	1800		in diffuse emission
35	WC6	900	5	new ring
35a[1]	WN6	900	6	new ring
35b[1]	WN4	900	7	possible ring, in cluster
36	WN4	900	8	new ring
38a[1]	WN6	900		
38b[1]	WC7	900		
42a[1]	WN4.5	600		In NGC3603.
42b[1]	WN3+C	600		ditto
42c[1]	WN6	600		ditto
42d[1]	WN4	900	9	ring near NGC3603.
44a[1]	WN3	900		diffuse emission
47	WN6+O5	900		
48	WC+O9I	900		
48a[2]	WC8	900		
66	WN8	900		
81	WC9	900		
82	WN8	900		
94	WN6	900	10	new ring.

All star names are from the catalog of galactic WR stars by van der Hucht *et al.*, (1981) except:

[1] from Shara *et al.*, 1991.

[2] from Danks *et al.*, 1983.

Table 2: Synopsis of results for observed optical emission-line nebulae in the complete southern hemisphere survey of WR environments.

WR #	WR type	b	Distance (pc)	Ring type	Diameter (′)	Diameter (pc)
6	WN5	-10.08	1000	E	40	11.6
7	WN4	-0.13	3900	W/E	5	5.7
11	WC8+O9I	-7.69	300	E	57	5
14	WC7	-1.64	1800	R	34	17.8
16	WN8	-2.55	2600	W/E	8	6.1
18	WN5	-0.97	2000	W/E	17	9.9
20	WN4.5	-1.84	5900	R	43	73.8
20a[1]	WN7	-0.34	2300	W	7.3	4.9
20b[1]	WN7	-0.35	2300	W	4.1	2.7
22	WN7+abs	-0.85	2100	W?	11	6.5
23	WC6	-0.03	4300	R	30	37.5
30	WC6+abs	-2.61	5700	W/E	10	16.6
31	WN4+O7	0.02	4300	E	7	8.8
32	WC5	0.02	22400	R	27	176
35	WN6	-1.18	16000	R	25	117
35a[1]	WN6	-0.06	8300	R	10.3	24.9
36	WN4	0.56	4400	R	18	23.0
38[a]	WC4	-0.92	3100	E?	24	21.6
40	WN8	-4.83	2200	W/E	9	5.8
42	WC7+O5-7	-0.49	2300	E	15	10
42d[1]	WN4	-0.48	2800	W/E	2.5	2.0
43	WN7+abs	-0.52	2200	W	2	1.3
52	WC5	4.55	2100	R	60	36.7
54	WN4	-2.5	6100	R	20	35.5
55	WN7	0.16	5500	R	39	62.4
57	WC7	-5.03	4000	E?	16	18.6
60	WC8	0.74	4500	E?	18	23.6
65	WC9	-1.2	2100	W	15	9.0
68	WC7	-1.88	3000	W/E	15	13.0
71	WN6	-7.61	11000	E	9	28.8
75	WN5	-1.48	3960	W	9.5	20.7
77	WC8(+abs)	-1.09	1100	W	8	2.6
85	WN6	-0.61	3700	W/E	9	9.7
87[b]	WN7	-0.77	1300	W?	23	8.7
91	WN7	-1.07	7400	W/E	20	43.1
93	WC7+abs	0.83	1100	W	9	2.9
94	WN6	-0.25	5400	E	11	17.3
98	WC7/WN6	-0.87	2400	W/E	10	7.0
101	WC8	-1.43	6900	W/E	16	32.1
102	WO1	1.41	4900	W	8	11.4

All distances from Conti & Vacca (1990) except: [1] Shara *et al.*, 1991.

[a] nebula surround WR37, WR38 and WR39.

[b] nebula surrounds WR87 and WR89.

Figure 1: $H\alpha$ image of the region around WR20 (shown by a cross). The image is $31'$ across. A partial shell is seen to the north of the image.

Figure 2: $H\alpha$ image of the region around WR20a and b in the Westerlund 2 star cluster. The image is $15.5'$ across.

Figure 3: View of the partial shell to the east of WR20a and b and the Westerlund 2 star cluster.

Figure 4: Image of the cleared out region around WR32. The shell is $27'$ across.

Figure 5: New $25'$ ring observed around WR35. The image is $31'$ across.

Figure 6: New shell around the star WR35a. The image is $15.5'$ across.

Figure 7: A partial shell observed around the star WR35b. The image is $31'$ across.

Figure 8: New, complete shell around the star WR36. The star is off-center, towards the eastern edge of the shell.

Figure 9: Small ring associated with WR42d. The star is close to the complex HII region, NGC3603. The image is $7.7'$ across.

Figure 10: Weak ejecta shell associated with WR94. The image is $15.5'$ across.

Figure 11: The detection rate of nebulae associated with WR stars as a function of galactic latitude, b. A slight increase in detections is noted for objects at the smallest galactic latitudes.

Figure 12: The distribution of the derived nebula diameters of types W and/or E for each of nebulae associated with the WR subtypes, WN and WC.

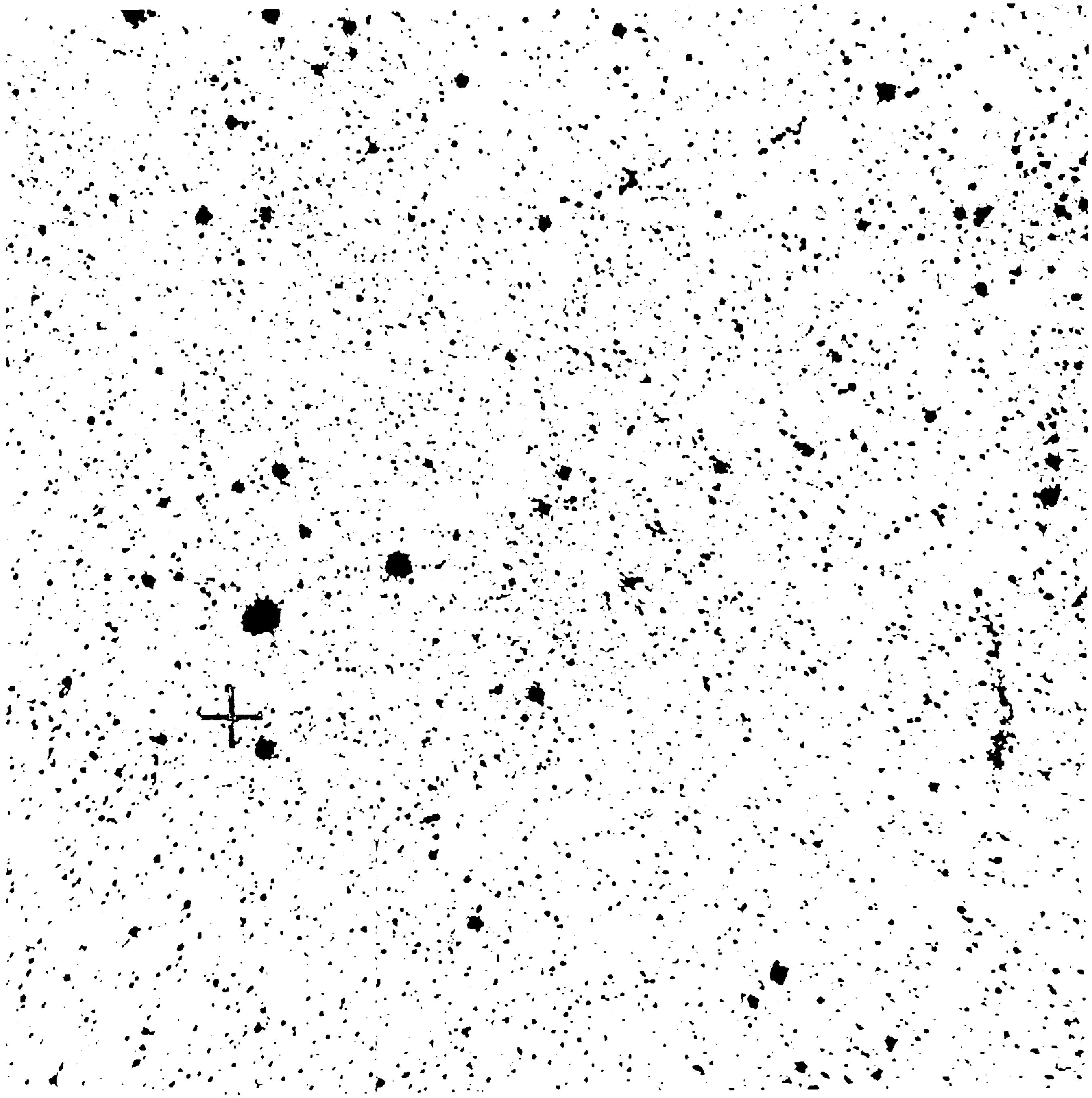

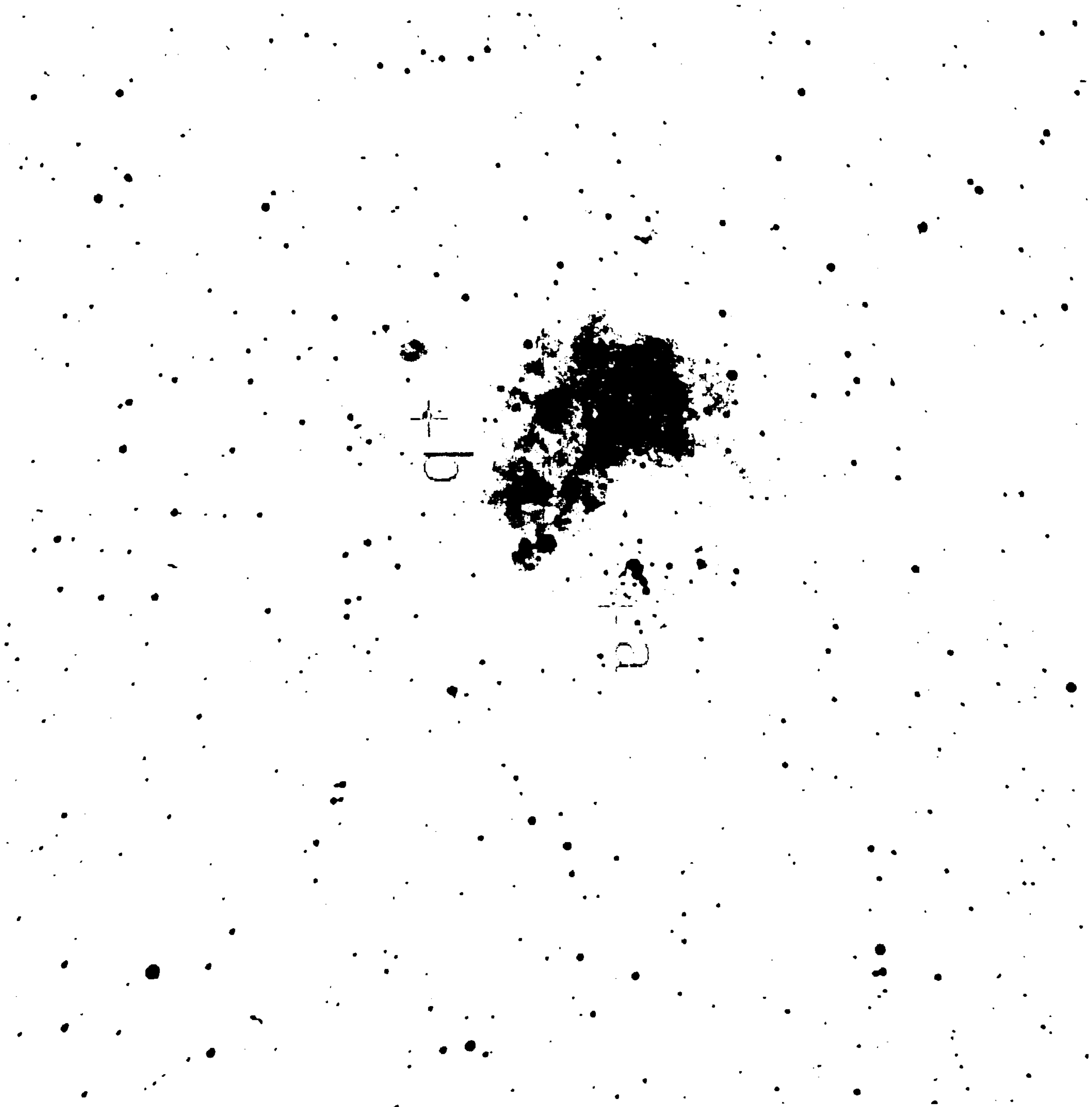

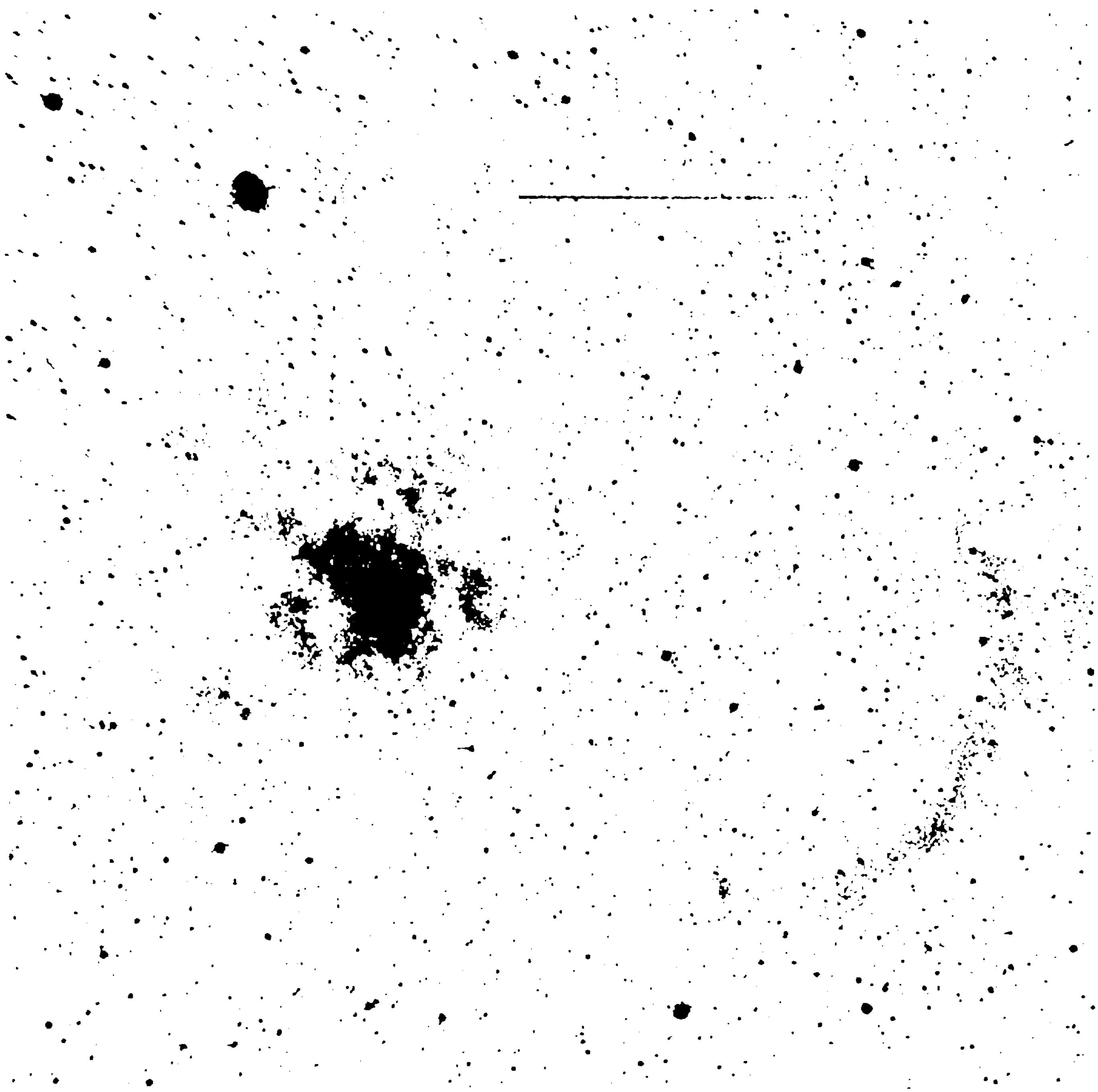

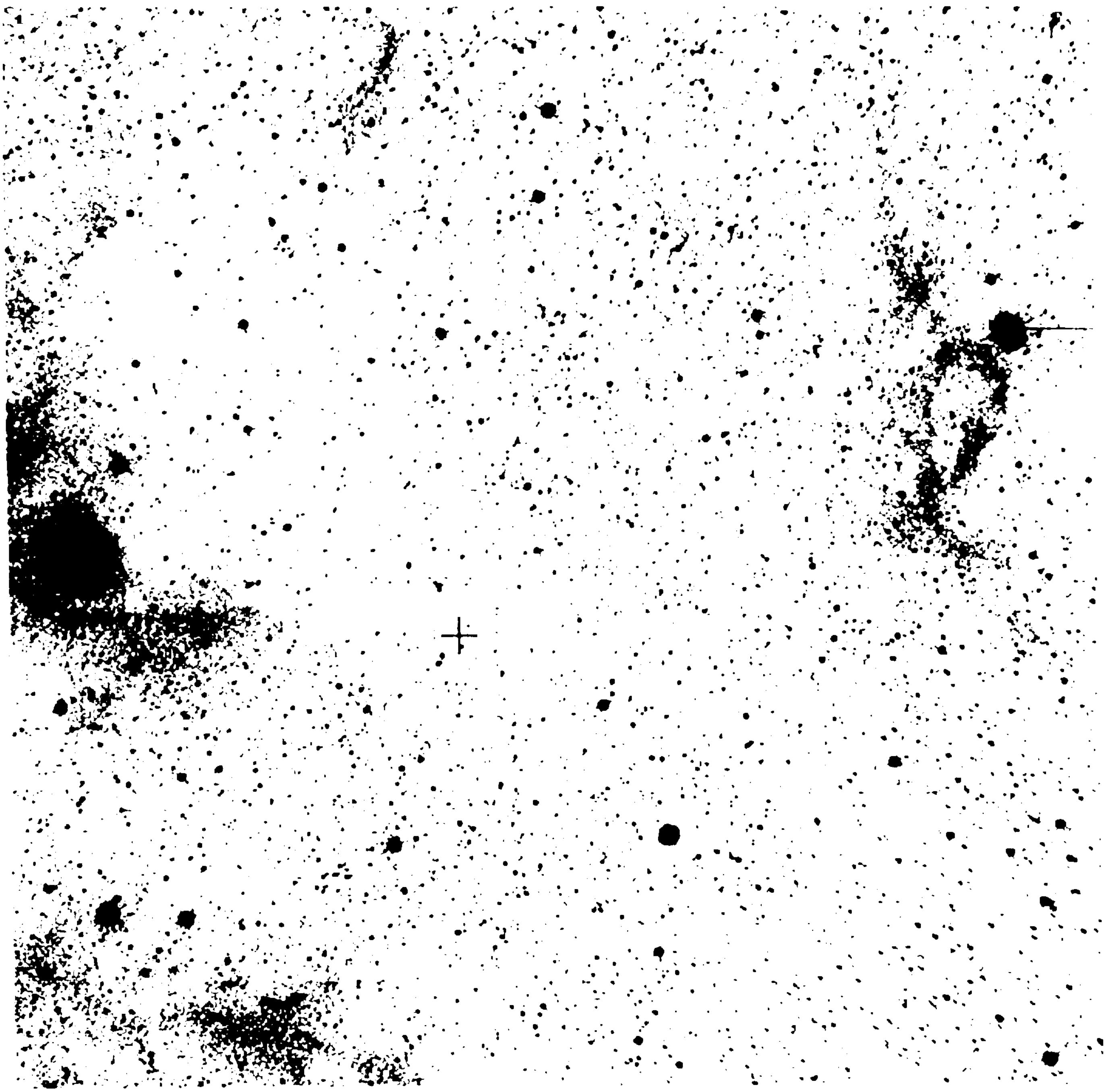

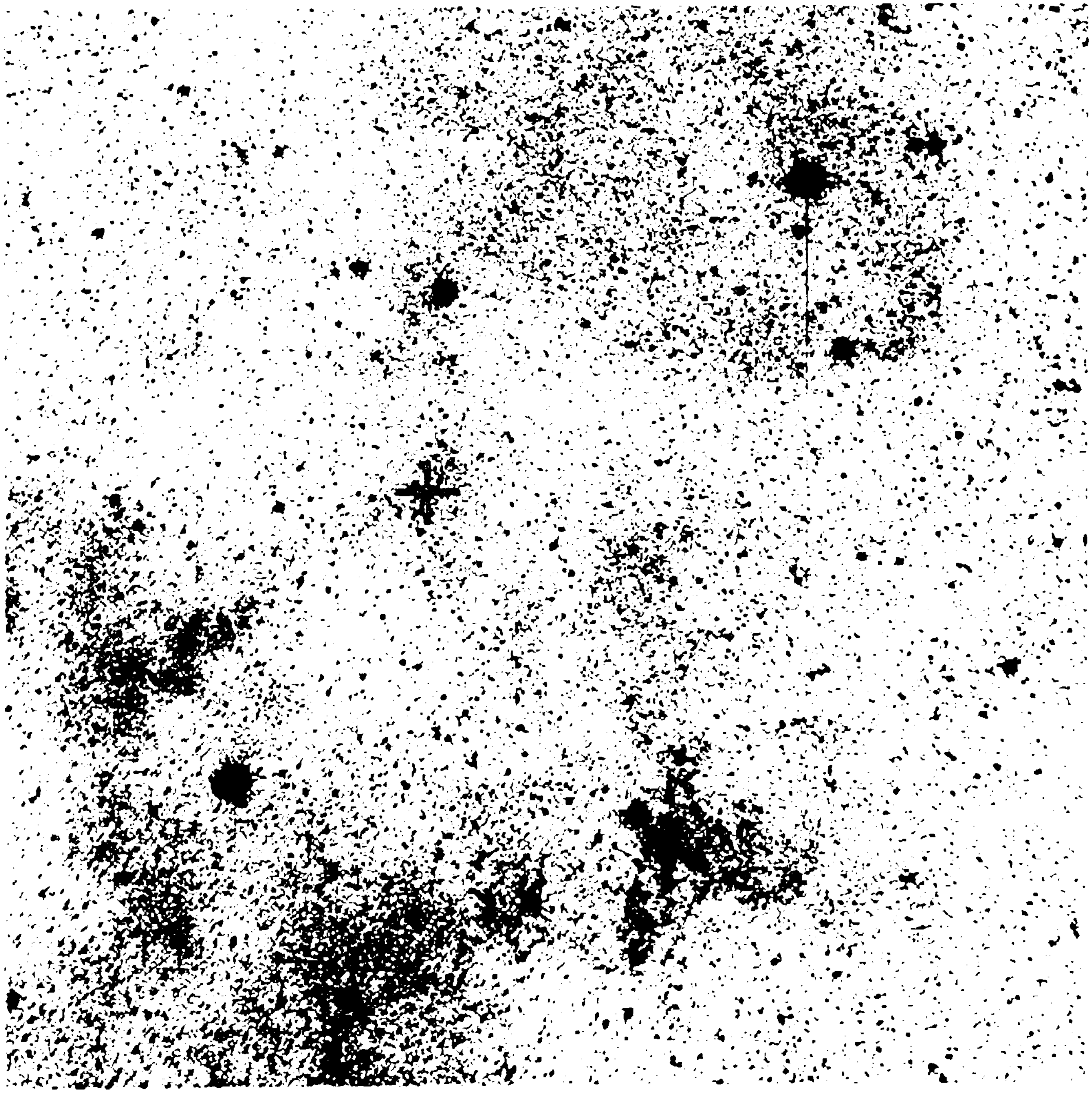

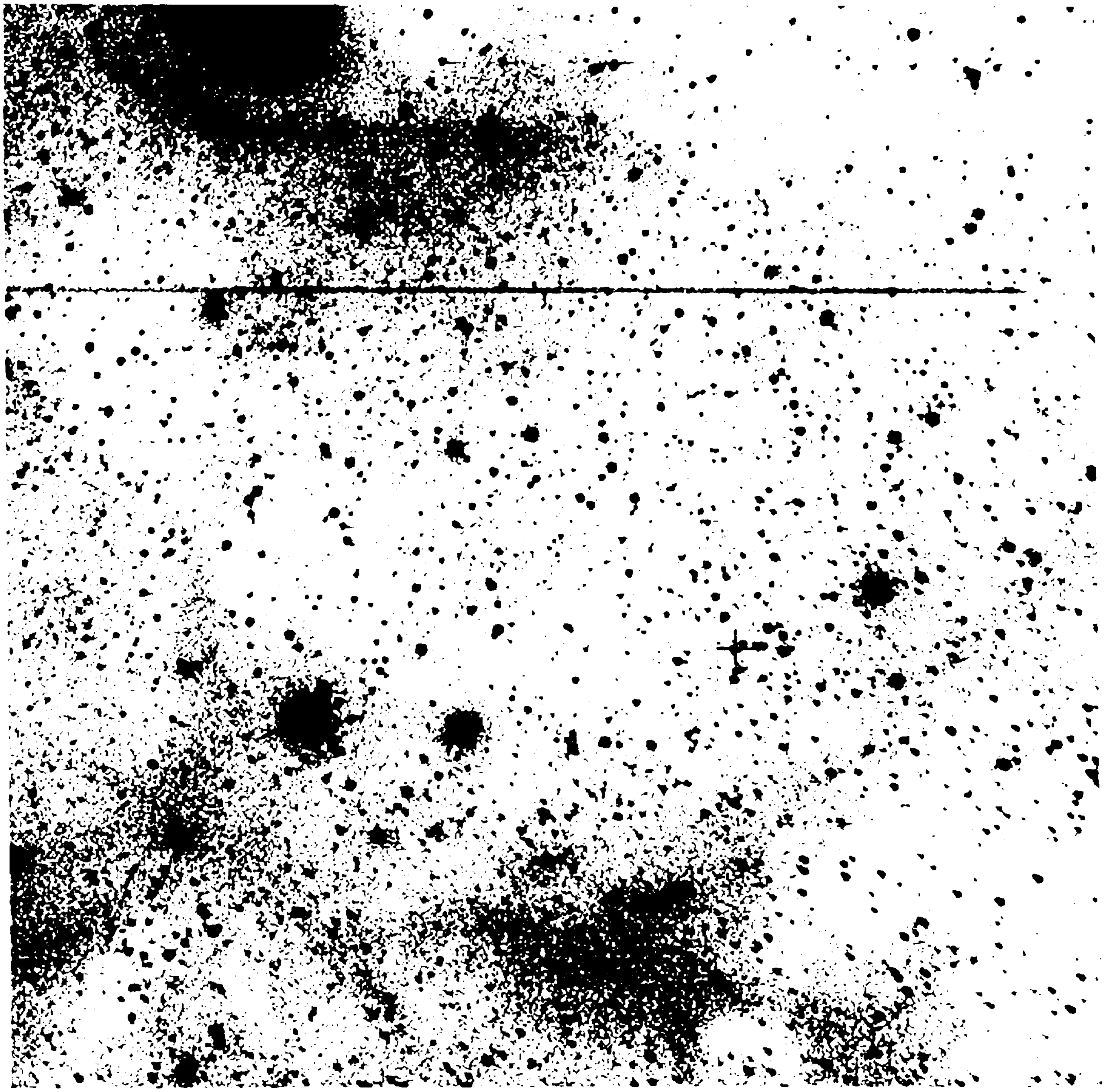

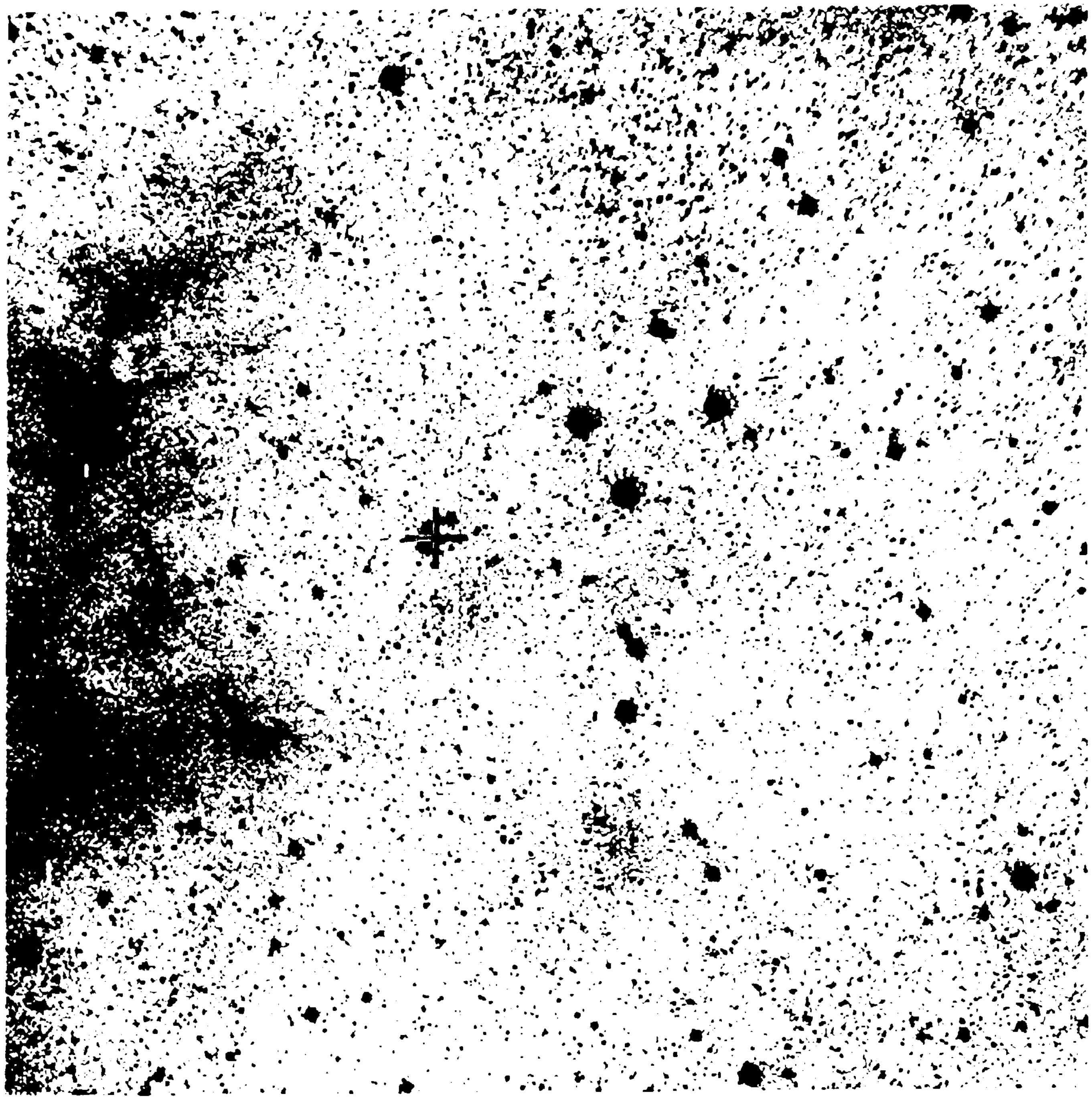

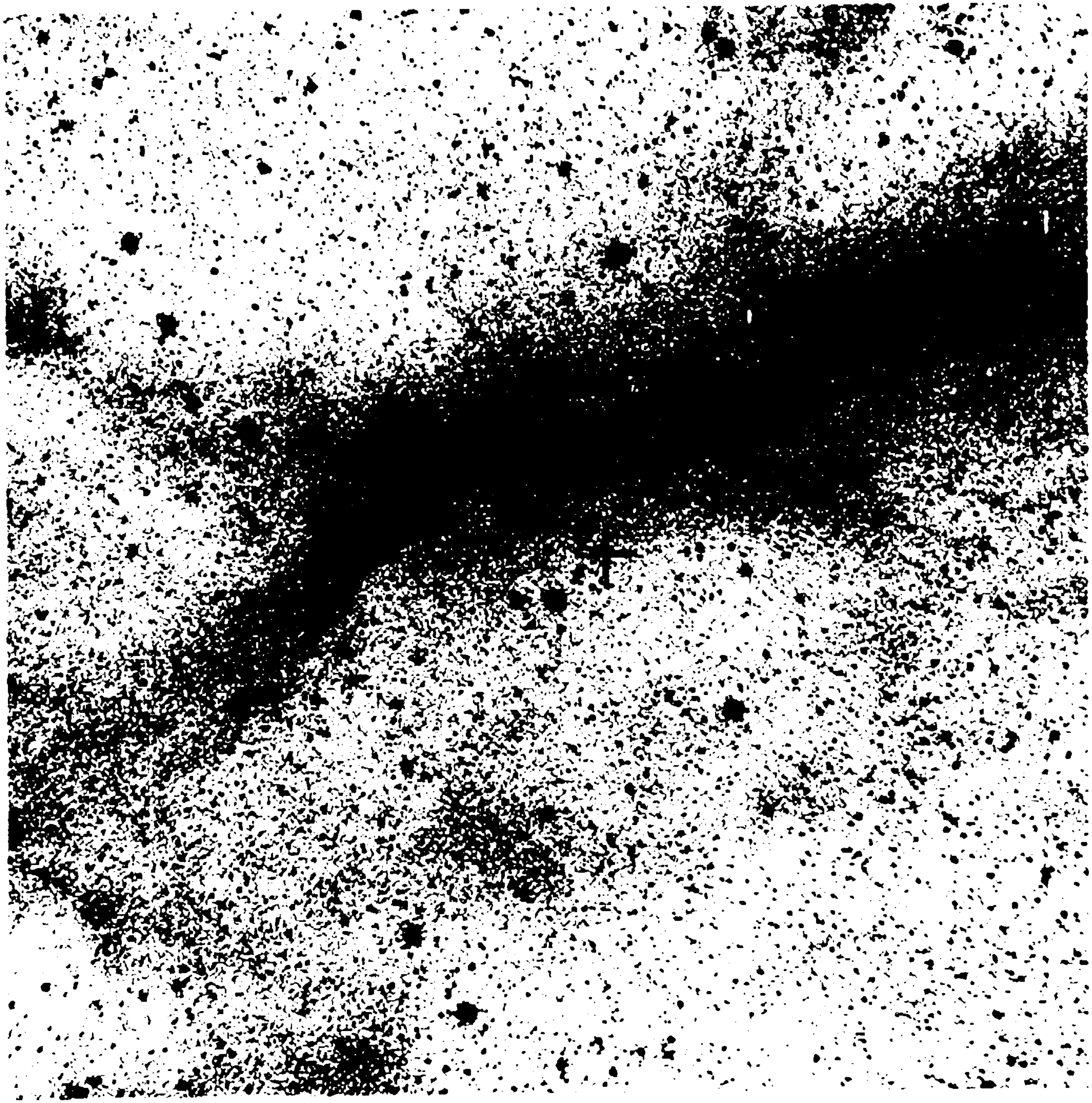

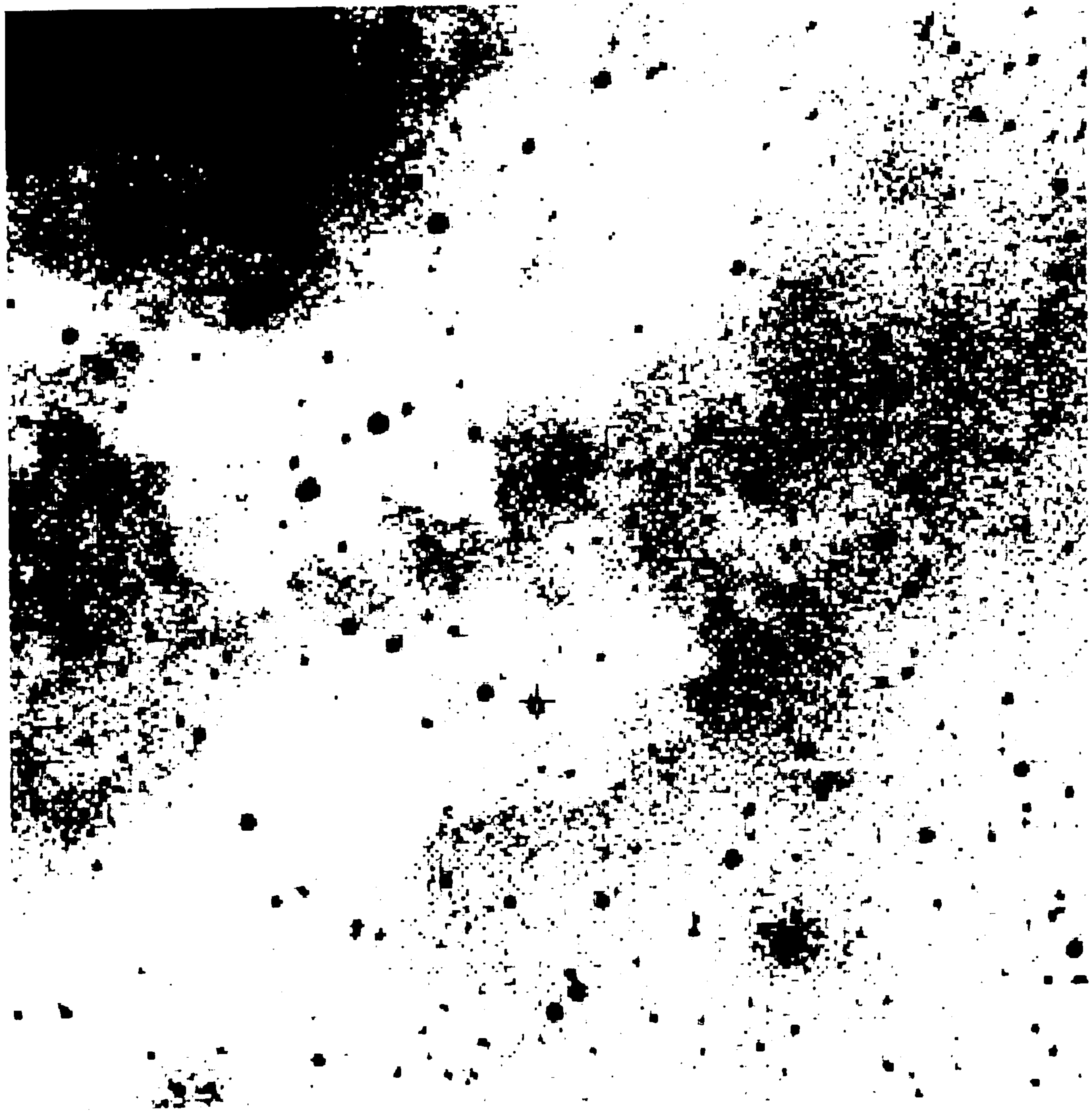

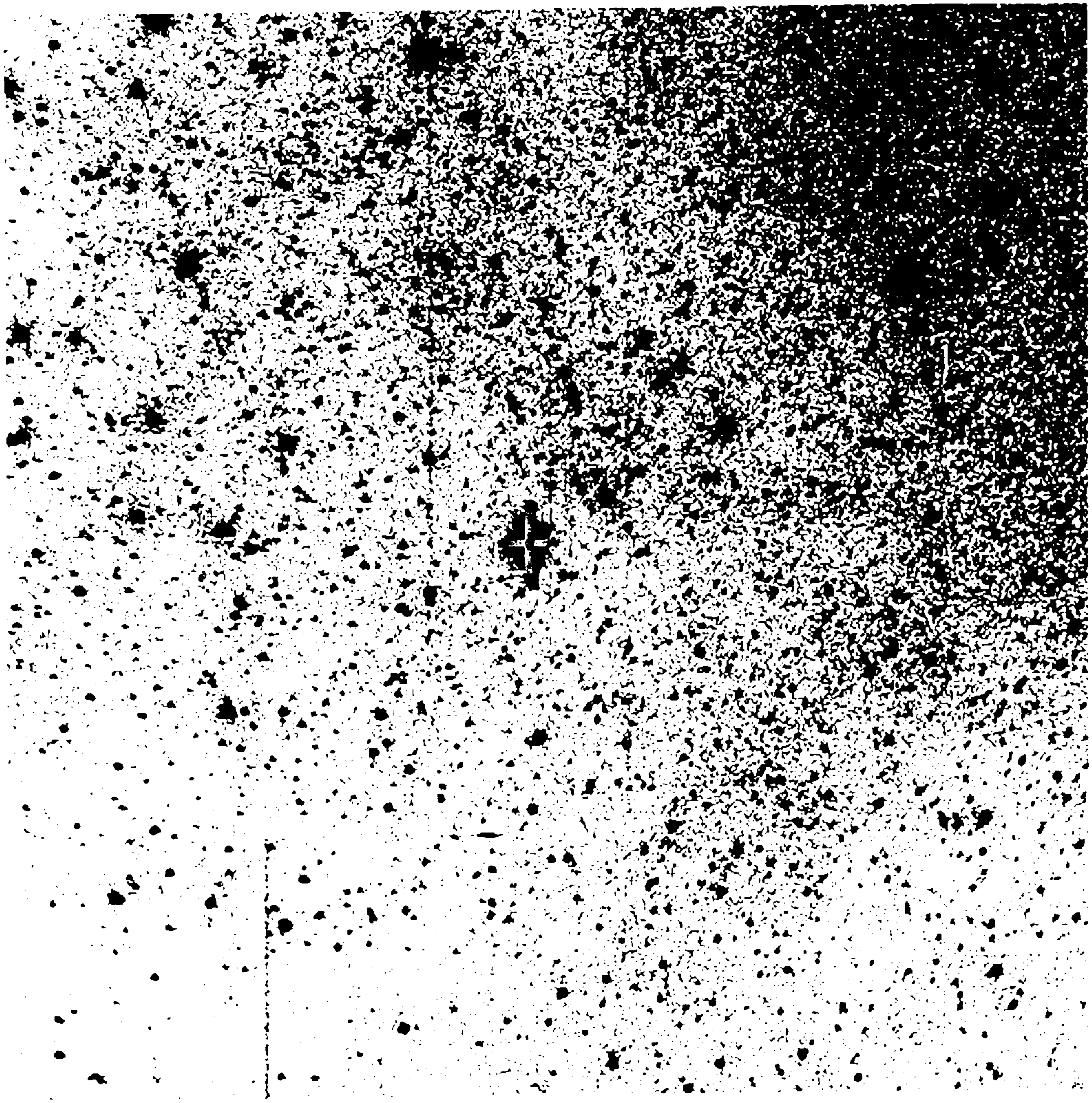

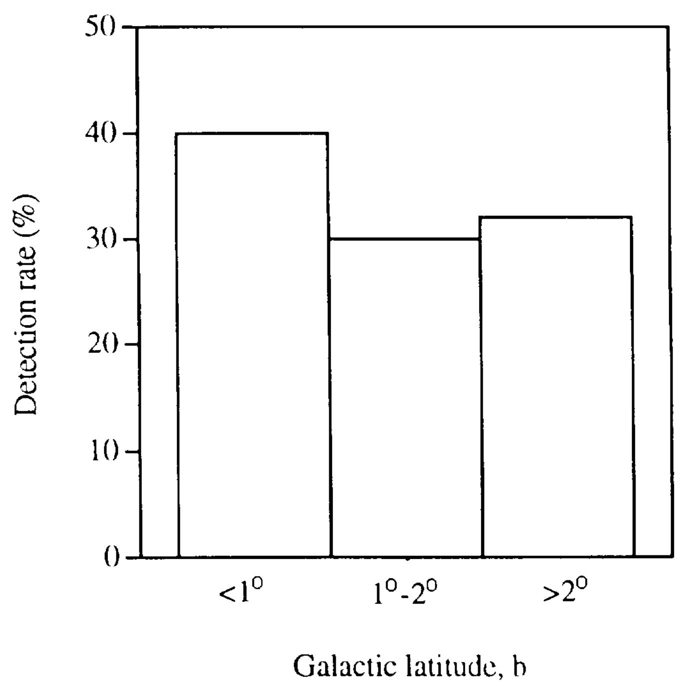

50
40
30
20
10
0
Detection rate (%)
<1°
1°-2°
>2°
Galactic latitude, b

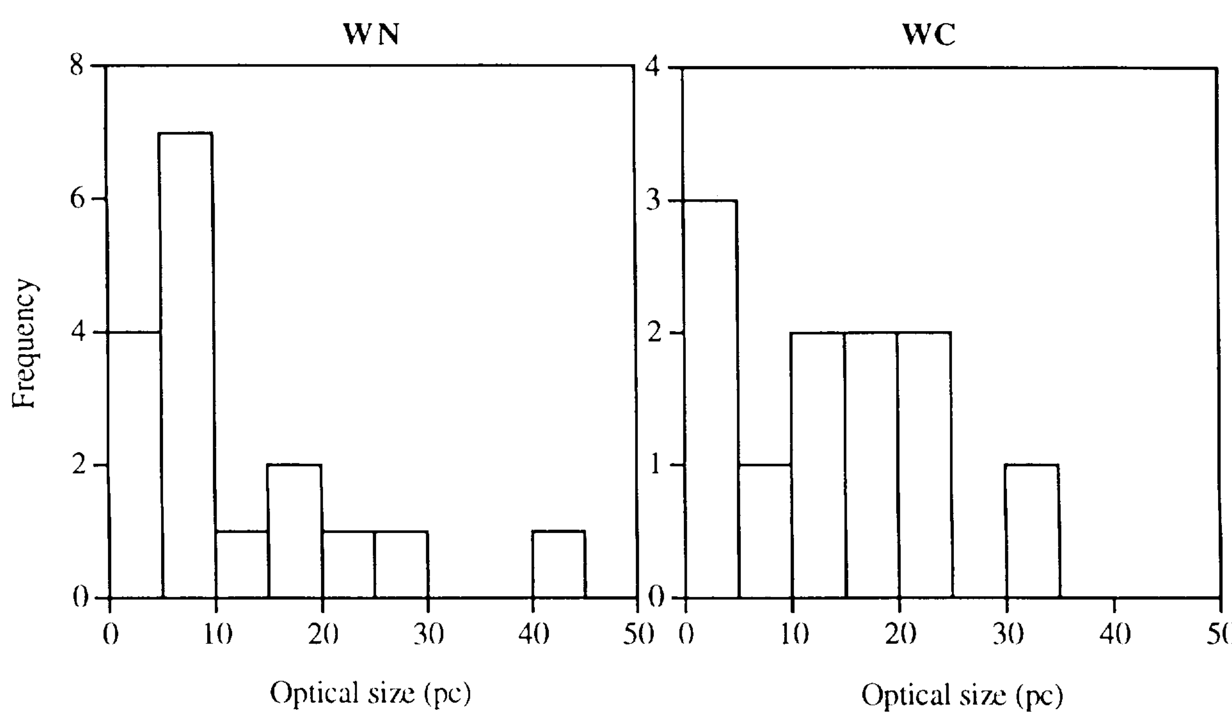
WN
WC
Frequency
0
2
4
6
8
0
1
2
3
4
0
10
20
30
40
50
Optical size (pc)
Optical size (pc)

Large IRAS Shells Around Galactic Wolf-Rayet Stars and the O Star Phase of Wolf-Rayet Evolution

A. P. Marston

Dept. of Physics & Astronomy, Drake University, Des Moines, IA 50311

Submitted to the Astronomical Journal.

Abstract

We present IRAS Skyflux images of the environments of galactic Wolf-Rayet stars. These form a complete sample of all galactic Wolf-Rayet stars of the van der Hucht *et al.* (1981) catalog observed by IRAS, a total of 156 stellar environments. The intent of this survey is to obtain information on the large bubbles expected from the early O star phase of Wolf-Rayet stars. A total of 49 probable or suspected shells of $>20'$ in diameter have been observed in our data, with a detection rate of 60% for large IRAS shells around Wolf-Rayet stars at galactic latitudes $>2°$. Fourteen of the IRAS shells are associated with previously observed, slowly expanding HI bubbles. Most shells are unlikely to be due to line-of-sight coincidence, although two shells may be associated with foreground or background supernova remnants. In considering the origin of the shells we indicate that most are unlikely to have formed from a the explosion of a binary companion to a Wolf-Rayet star and that few, if any, are likely to be associated with ejecta produced in a Roche Lobe overflow. The sizes of the shells, together with their known or estimated expansion velocities are consistent with the estimates of the period of the O star progenitor phase calculated in evolutionary models of single WR stars.

1 Introduction:

In the past few years a number of Wolf-Rayet (WR) stars have been observed as having multiple, concentric rings of material around them (Dopita et al., 1994; Marston, 1995a). In Marston (1995a) it was shown how such multiple shells are likely to be indicative of several phases of evolution of WR stars, as they evolve from their O star progenitor state. A three phase evolution, starting with an O star proceeding through a high-mass loss phase (e.g. Luminous Blue Variable) and continuing to the WR star phase, is consistent with the optical and infrared data presented on nebulae around WR stars (Marston, 1995a; Marston, 1995b). The most recently ejected/swept up material is observed closest to the stars and can frequently be observed in narrow-band imaging (Miller & Chu, 1993; Marston *et al.*, 1994a; Marston *et al.*, 1994b). These shells of material are associated with a heavy mass-loss phase followed by a strong stellar wind phase which occurs in the WR phase of the star. Further out from a WR star resides a shell of swept up interstellar medium possibly associated with the stellar wind of the star during its O star progenitor phase. Although occasionally observed optically around WR stars (approximately 8% of all WR stars show such extended shells optically, Marston, 1996), such shells are expected to be of predominantly cool material and may be more readily observed at far-infrared wavelengths or using radio/sub-mm emission lines of atomic or molecular gas. As an example, the WR star WR136 (numbering from van der Hucht *et al.*, 1981) is surrounded by multiple shells of material, with a large outer ring seen using IRAS Skyflux (Nichols-Bohlin & Fesen, 1993) and IRAS high resolution (HIRES) data (Marston, 1995b). A number of WR stars have been shown to be inside of large HI bubbles of similar dimensions to that around WR136 (Arnal, 1992; Cappa de Nicolau & Niemela, 1984; also see Marston, 1995b and references therein).

It was shown in Marston (1995b) how the sizes of the concentric shells associated with the O star phase, ejecta phase and WR wind phase, plus information on their expansion velocities could provide time scales for each part of a three phase evolution for WR136. While estimates of total mass loss from the central WR star in the final phases could be estimated based on IRAS fluxes of the ejecta shells. The mass of swept-up material in extended IRAS shell may also be estimated using IRAS fluxes, which Marston (1995b) associates with a bubble created by the O star progenitor of WR136.

An alternative view to the creation of large IRAS shells around WR stars has been put forward by Nichols & Fesen (1994). They suggest two creation schemes that involve the evolution of binary WR stars. The large IRAS shells may arise from the supernova explosion of a binary companion to a WR star, or from ejecta during a Roche Lobe overflow from the WR star progenitor onto a compact companion.

In order to obtain more information on the evolution of WR stars, we have embarked on an IRAS survey of galactic WR stars. This has involved a survey of IRAS Skyflux data associated with the environments of WR stars (providing information on large shells), plus a complementary survey program of HIRES IRAS data (Aumann *et al.*, 1990), for more detailed analysis of smaller shells and mass-loss associated with stellar ejecta.

In this paper we present the findings of our Skyflux survey of the regions around 156 galactic WR stars using IRAS Skyflux data at $12\mu m$, $25\mu m$, $60\mu m$ and $100\mu m$ wavelengths. The intent of this survey is to find large (>20′) shells associated with galactic WR stars. In the following sections we describe the data used and the results of the analysis of the Skyflux fields. We discuss the formation of the large shells via both WR binary and single star evolutionary modes. From the sizes of the IRAS shells observed, their statistical frequency and the (limited) knowledge of their dynamics we determine the most likely origin of large IRAS shells and what they can tell us about the evolution of the WR stars they surround.

2 Data Used:

We have surveyed the fields of 156 galactic WR stars of the catalogue of van der Hucht *et al.* (1981) using IRAS Skyflux data, which consists of images made of the sky at wavebands centered on $12\mu m$, $25\mu m$, $60\mu m$ and $100\mu m$. The two stars WR72 and WR99 in the catalog of van der Hucht *et al.* (1981) were omitted as they are not now classified as WR stars. Each region investigated was of 6 degrees square centered on one of the 156 galactic WR stars. Our survey therefore provides coverage of approximately 84% of all known galactic WR stars at mid- and far-infrared wavelengths (van der Hucht, 1994).

Evidence for large shells (>20′) was searched for around each of the stars in the survey. Structures of complete or partial shells apparently centered close to or on the position of the WR star were deemed associated with the star. In certain cases, the association was corroborated by previously obtained optical images or HI data. Size estimates were made via a fitted ellipse to the observed shell structure.

In certain cases, estimates of the far-infrared fluxes associated with the large shells were possible from the data. The flux interior to an ellipse around each shell was obtained and a local background external to the ellipse removed to obtain these fluxes.

3 Results:

A total of 49 probable shells associated with WR stars were found with diameters greater than 20′ in the IRAS Skyflux data (see Table 1). Of these, 2 were previously noted by Nichols-Bohlin & Fesen (1990; 1993) and one by Dubner et al. (1990). This provides an overall detection rate of 31%. Images of each of the associated IRAS nebulae are provided in Figs. 1. Fourteen of the observed IRAS shells correlate with previously observed HI cavities around WR stars, and are indicated in Table 1. In each of these case, the structure of the faint IRAS rings mimics that of the HI holes. HI velocity information confirms the fact that the shells are expanding about the central WR stars. The HI structure around WR125 (Arnal & Mirabel, 1991) is not obvious in the Skyflux data, although an extended source centered on the star is seen. A nearby pulsar, at the same distance as WR125 has prompted Arnal & Mirabel (1991) to associate the extended HI structures with a supernova remnant which extends around WR125, possibly originating from a high mass binary companion.

Using the distance data of Conti & Vacca (1990), physical size estimates of the large IRAS shells can be obtained, based on their average diameters. These show a range in diameter from 10pc to 338pc (see Table 1). In the case of some nearby WR stars, the observed shell may be associated with a WR wind-blown bubble (W) or ejecta (E) phase.

This is certainly the case for the nebula around WR11. The largest shells, around WR33 and WR73, may well be associated with supernova remnants, as these are in the same directions as pulsars PSR 1056-57 and PSR 1609-47 respectively (although at significantly different distances). In considering the positions of 330 pulsars listed in Manchester & Taylor (1981), no other pulsars appear interior to the observed IRAS shells.

The number of large shells observed in the IRAS Skyflux data is affected by galactic latitude. Fig. 2 shows how the detection rate for the observed shells changes with galactic latitude. At the higher latitudes, the detection rate increases quite steeply and 2/3 of all WR stars above a galactic latitude of 2° are observed to have shells larger than 20′. This suggests that the main cause of non-detection is the confusion of IRAS shell sources in the galactic plane. Also, large shells in the plane of the galaxy are more likely to be disrupted through interaction with other wind-blown or supernova remnant shells. Small shells are unlikely to be observed in regions high above the plane of the galaxy, since the low densities of the interstellar medium lead to small shell masses and IRAS intensities that are too low for the large IRAS shells to be detected. A weak trend of increasing shell size with galactic height can be observed in Fig. 3.

IRAS fluxes were obtained for 10 shells while further IRAS flux data was obtained for the extended shell around WR136 from Marston (1995b). The IRAS fluxes observed from the shells are listed in Table 2. Typically, the accuracy of the fluxes measured are, at best, within 20%. This is mainly due to the varying background in the large areas over which the shells are observed. In the 14 cases of HI cavities observed around WR stars, the swept-up HI masses (adjusted to the distances quoted by Conti & Vacca, 1990) are presented in Table 3, along with derived gas masses from IRAS data (based on the model of Marston & Dickens, 1988). It should be noted that total gas mass estimates based on IRAS data are notoriously inaccurate (see Mathis et al., 1992) and with the inaccuracy of the IRAS flux measurements the IRAS gas mass estimates are probably only slightly better in accuracy than an order of magnitude. In the two cases where HI measurements coincide with IRAS measurements, the IRAS measurements suggest gas masses that are factors of 1.1 and 3.6 higher than the HI gas masses respectively. However, the total gas mass in IRAS shells may well be higher than the HI masses as molecular material might also be expected to exist in the swept-up shells.

If we assume the shells are formed from swept-up interstellar medium, then using the shell sizes from Table 1 together with the estimated gas mass enables estimates of the original particle density local to the WR stars to be made. These results are also presented in Table 3.

An inverse relation is noted between shell size and the calculated local density of the interstellar medium (Fig. 4). Shells with diameters of 100pc or more are associated with low-density surroundings. This is in part due to penetration of such shells out of the densest parts of the galactic disk. Overall, the shell diameters are expected to also be functions of the wind luminosity and the age of the central WR star.

Overall, the detection rates for shells surrounding the WR subtype WN and WC stars are 32% and 31% respectively (for rings larger than 20′), while 2 of 6 WN/WC type stars showed such shells, suggesting no bias towards large shell formation around a particular subtype.

4 Discussion:

The origin of large IRAS shells apparently associated with WR stars has been a subject of some debate. Line-of-sight coincidence appears unlikely given the connection with HI features with similar kinematical distances as the central WR stars (e.g. Arnal, 1992). The central location of most stars in the IRAS shells also argues strongly against many coincidences.

In Nichols & Fesen (1994), two main alternatives were put forward for explaining the extended shells around WR6, WR40 and WR136 (each of which has a bright optical ring nebula interior to a large IRAS shell). Their first suggestion is that large IRAS shells are supernova remnants associated with the explosions of binary companions to the WR star. Alternatively, Nichols & Fesen (1994) suggest that material ejected during a Roche Lobe overflow (RLOF) from a WR progenitor onto a compact companion forms the large shells. We now consider these two alternatives as well as the origin of large IRAS shells as interstellar matter swept-up during the O star progenitor phase of WR stars.

4.1 Supernova Origin

In this alternative, the extended shells are created from an exploding primary companion at or just before the point where the WR star first becomes a WR star. Nichols-Bohlin & Fesen (1993) suggested that the large (1.7° x1.5°) shell surrounding WR136 is associated with a supernova explosion in the neighborhood of the WR star. This conclusion was based in part on the low Hα/[SII] emission-line ratio seen in optically observed filaments apparently associated with the shell. However, the physical connection of these filaments to the IRAS shell is not clear. They may well be associated with supernova material in a super-association, either foreground or background to the IRAS shell, perhaps associated with high-velocity UV absorption lines observed in the region (St-Louis & Smith, 1991). The high-velocity features appear to extend beyond the large IRAS shell and it is unlikely that there is a direct connection between the IRAS shell and these high-velocity absorption features.

For the shells around WR6 and WR40 Nichols & Fesen (1994) suggest that the large IRAS shells are associated with high-velocity absorption features observed in the UV leading to the possibility that the large IRAS shells are either supernova remnants with ages of 10^5 years, or a similar aged nebula created during a RLOF (see Section 4.2). WR6 and WR40 are 2 of 35 stars with IUE observations analysed by Nichols & Fesen (1994). Of these 35 WR stars 43% observed as having high-velocity absorption lines are observed by us to have extended IRAS shells, while 50% of those having no associated high-velocity absorption lines also have IRAS shells. The IRAS shell around WR148 is also noted in HI with an expansion velocity of around 6kms^{-1} (Dubner et al., 1990). High-velocity absorption lines are also noted in the spectrum of this star. All this leads us to conclude that there appears to be little correlation between the existence of high-velocity absorption line features and that of a large IRAS shell. Indeed, all 14 of the HI observed large IRAS shells have expansion velocities of 20kms^{-1} or lower, which are far smaller than the velocities of the absorbing materials observed in the

WR spectra.

We conclude that it is unlikely that supernova remnants are the main origin of large IRAS shells around WR stars. Indeed, we further note that none of the IRAS shells surround both a pulsar and a WR star.

4.2 Mass Ejection due to Roche Lobe Overflow

In this mechanism, a WR star and an OB star exist in a binary. The supernova explosion of the WR star creates a compact companion, which will remain bound if the star system becomes a "runaway". This scenario has the advantage of enabling WR stars to move out of the galactic disk to large distances (>100pc) above the galactic plane while the O star ages. The O star then evolves towards being a WR star over a period of several million years. As it expands, following the depletion of H in its core, material can flow (RLOF) onto the compact companion at a rate exceeding the Eddington limit. This leads to a mass ejection which Nichols & Fesen (1994) suggest produces the large IRAS shells. This ejection leads to shells expanding at high velocities, as indicated by the high-velocity UV absorption lines. The ages of such shells should be approximately 10^5 years.

In Section 4.1 it was indicated that high-velocity UV absorption lines have no obvious connections to the existence of large IRAS shells around WR stars. Also, all shells so far observed using HI measurements exhibit expansion velocities of a few to 20 kms^{-1} (see Marston, 1995b and references therein). The expansion ages of these large shells are therefore of a few million years (see Table 3). This is a magnitude too large for the proposed RLOF mechanism.

The RLOF mechanism nicely explains the existence of runaway WR stars above the galactic plane, however, 11 out of 14 HI observed, large IRAS shells noted in this paper have distances away from the galactic plane of more than 100pc and may be considered potential runaway stars. None of them show the fast expansion velocities.

Although some WR stars are suspected of having compact companions, the numbers are likely to be small. Yungelson & Tutukov (1991) predict that up to 10% of WR stars may have close compact companions, and Vanbeveren (1988) indicates that the number of WR stars with compact companions is likely to be less than 5%. Vanbeveren (1994) also indicates that the likelihood of a bound system after an initial supernova is low due to the large kick velocities involved. But more than 30% of our WR sample show large IRAS rings. It appears unlikely that as many as one third of the galactic WR population, that are observed as having large IRAS shells, would have the compact companions necessary for the RLOF picture to be the primary mechanism for large IRAS shell creation. Further, six stars noted as being in WR+OB binaries also have large IRAS shells. It appears certain that no supernova or RLOF phase can have caused the shells associated with these objects.

It therefore appears unlikely that many (if any) of the large IRAS shells are created during a RLOF onto a compact companion to a WR star.

4.3 Wind-blown Bubbles

Nichols & Fesen (1994) suggest that the large IRAS shells existing around WR6 and WR40, which are well out of the galactic plane, are inconsistent with the fact that similar structures are not to be seen around stars in more dense environments. Our survey indicates that such shells do exist for objects in the galactic plane but are less often observed as such due to confusion. A distinct increase in the detection rate of observed large shells is seen at high galactic latitudes (see Fig. 2). Also, in Fig. 3 we showed that the extended IRAS shells are distinctly smaller at small galactic heights, making them less likely to be observed by IRAS as highly extended objects. Marston (1996) has also shown that the detection of optical ring nebulae appears to be independent of galactic latitude, suggesting that the existence of an optically observed ring nebula, usually of an ejecta or wind-blown type, depends on the evolution of the WR star (particularly in its heavy mass-loss, ejecta phase) rather than on its environment.

In Marston (1995a) it was illustrated how multiple optical ring nebulae around WR stars are consistent with a three stage WR evolution from an O star, through a heavy mass-loss phase to becoming a WR star. Marston (1995b) also illustrated that the nebulae associated with WR136 are consistent with this picture. In this case the large IRAS shell associated with WR136 is consistent with a wind-blown O star progenitor shell with an age of around 2 million years, a value typical of the total age of the more massive WR stars (Maeder & Meynet, 1994). The inner, optically observed ring nebula (NGC6888) is then interpreted as being associated with an ejecta shell being penetrated by a wind from WR136.

If we make similar assumptions to Marston (1995a), we are able to obtain estimates of the shell ages and therefore the lifetimes, t_{WR}, of the associated WR stars from the radius, r, and the velocity of expansion of the large IRAS shell, v_{exp},

$$t(yrs) = \frac{10^6 r(pc)}{v_{exp}(kms^{-1})}. \qquad (1)$$

Only a few of our objects have known expansion velocities (see Table 3). Taking an average expansion velocity of 10kms^{-1} for the rest of our sample indicates timescales of 0.65 to 16 million years. However, the upper limit is imposed by two observations that may be confused with supernova remnants associated with pulsars in the same line of sight (shells around WR33 and WR73). Removing these leaves an upper limit of 14 million years. It is also possible that some of the smaller shells observed are actually associated with the ejecta phase of the star (we will deal with these in our IRAS HIRES survey). Within the errors associated with our calculation (factors of 2), the lifetime of these stars in an O star phase is consistent with estimates from models of single massive star evolution (Maeder & Meynet, 1994). A distribution of the ages associated with the large IRAS shells is presented in Fig. 5. Most stars have ages in the range of 1 to 5 million years.

In Fig. 4 it was illustrated that larger shells were generally produced in the less dense environments at 100pc and more away from the galactic plane. Fig. 6 illustrates that the observed IRAS shell time scales tend to increase with galactic height (z). This would suggest that less massive WR progenitor stars, with longer O star phases, are being observed at greater galactic height and more massive WR progenitors are observed in the galactic plane, in regions of higher gas density. Another possibility is that the WR stars formed at higher galactic latitudes have lower abundances and a longer O star progenitor phase (Maeder & Meynet, 1994). However, these results must be treated with some caution. As noted earlier, the detection of large IRAS shells is likely to be biased. At large z, the low density of the interstellar medium would make small IRAS shells difficult to distinguish above the background, while confusion in the galactic plane reduces the number of large IRAS shells observed at small z. The result of this being a lack of objects of smaller ages at large z and a lack of objects of larger ages at small z.

A three phase evolution model does not explain the high-velocity UV absorption line features observed in the UV spectra of some WR and nearby stars. Such absorption features do not appear to be directly related to the existence of extended IRAS shells, but what are they associated with? Goudis et al. (1988) showed the existence of optical emission-line, metal rich, high-velocity bullets of material in the shell surrounding WR75 (RCW104) which appear to be radiatively ionised nitrogen rich knots ejected from the WR star. Although this may explain high-velocity features associated with single massive stars, it does not explain the existence of similar absorption velocity features associated with other stars in the neighborhood of WR stars. Instead, extended high-velocity systems may well arise in super association shells (as suggested may exist outside the large IRAS shell around WR136 by Nichols-Bohlin & Fesen, 1993).

If the wind-blown bubble picture is correct, then the WR stars must presently reside very close to where they were created. In other words, they would need to be created in low gas density regions. However, Wood & Churchwell (1989) have shown the existence of ultracompact HII regions (UCHR), harboring newly born massive OB stars, well above the plane of the galaxy. The scale height for UCHR is 100pc, which can be compared to 45pc for the WR stars in our sample (Conti & Vacca, 1990). The creation of WR stars, forming in UCHRs, at distances of more than 100pc above the galactic plane is therefore reasonable.

The model associated with an O star progenitor bubble appears to fit the observational facts well. The large IRAS shells are of a size consistent with the observed, slow expansion velocities and have existed for a few million years, the expected lifetime of an O star progenitor. The existence of high-velocity UV absorption lines in WR spectra appears unconnected with these slowly expanding structures.

5 Conclusions:

We have presented the results of a study of IRAS Skyflux data associated with regions surrounding 156 galactic WR stars listed by van der Hucht *et al.* (1981). This catalog of WR stars is incomplete, as 185 WR stars are now known (van der Hucht, 1994). Most of the recently discovered galactic WR stars appear in stellar clusters, so our sample is somewhat biased against WR stars in regions of high densities. Of the 156 stars observed, 49 show evidence of large ($>20'$) shells. For objects above a galactic latitude of $2°$ the detection rate of large IRAS shells rises to over 60%. The frequency of observation of the new IRAS shells, particularly the sharp increase in the detection rate of shells around WR stars at higher galactic latitudes, suggests such large shells are quite ubiquitous, and only confusion with other sources and the galactic background of cirrus prevent a higher rate of detection in the plane of the galaxy. In 14 cases we find the IRAS shells coincident with previously observed HI shells. The central location and, in the 14 cases associated with HI shells, the kinematical association of the the IRAS shells with the central WR stars precludes line of sight coincidence for the majority of the shells. The existence of high-velocity features, seen in UV absorption lines towards WR stars (Nichols & Fesen, 1994), and sometimes seen in the spectra of neighboring stars, appears to have little correlation with the existence of a large IRAS shell associated with the WR star. The origin of these absorption features may be in larger super association shells (as suggested by Nichols-Bohlin & Fesen, 1993, for the UV absorption lines in WR136 and nearby stars).

The most likely origin of the large IRAS shells is the wind-blown bubble of the O star progenitor, although a supernova shell or a shell created from ejected mass from a compact companion during a RLOF have been suggested as origins for two previously known large IRAS shells (Nichols & Fesen, 1994). However, only two of our IRAS shells surround pulsars and in each case the pulsar is considered to be at a very different distance to the WR star. The shells, in these cases, may be foreground or background SNRs. No large IRAS shells surround both a WR star and a pulsar (although an HI shell around a WR star and pulsar has been observed by Arnal & Mirabel, 1991). It therefore appears as if there is no direct relation between the existence of the large IRAS shells and a supernova event. The likely percentage of WR stars with compact companions is also much lower than the observed large IRAS shell detection rate. This makes it unlikely that there are enough compact companions to WR stars in order for ejected mass from a RLOF to produce many, if any, of the large shells observed. The measured (and estimated) timescales for the expanding shells are too long for either the supernova or binary ejection models to work.

The cool outer rings produced in the O star phase of a WR have rarely been observed optically (only 8% of WR stars in a southern galactic survey show optical emission-lines which may be associated with the O star progenitor shells; Marston, 1996). The low temperature and large apparent sizes make them more easily visible in the IRAS data. Marston (1995b) has suggested that progenitor O star ring sizes may be used to estimate the ages of the central stars. Using similar assumptions, total ages of the 48 stars with associated O phase rings range from 0.5 to 16 million years (the IRAS shell around WR11 is almost certainly from an ejecta phase as it coincides with the optically observed ejecta shell; Marston et al., 1994b). The extreme values in ages are associated with shells for which an expansion velocity is not known and are likely to be uncertain by factors of 2. We conclude that our results are consistent with current estimates of the O star lifetime of single WR stars (Maeder & Meynet, 1994).

One consequence of associating IRAS shells with the O star phase is that, in order to remain central to the IRAS shells the WR stars close to their current position. This means producing some WR stars at heights of 100pc or more above the galactic plane. However, a number of ultracompact HII regions harboring young, massive stars exist at high galactic latitudes, and the scale height of these regions is greater than that of our WR sample. It appears likely that many WR stars have not moved far from their birthplace.

Further investigations of IRAS data of the regions surrounding WR stars will include a complete HIRES IRAS data survey of the catalog of galactic WR stars of van der Hucht *et* *al.* (1981). This will also allow the detection of the smaller ejecta and wind-blown shells around WR stars. The detected far-infrared shell sizes and total emission will enable the determination of the length of ejecta phases and total masses ejected by WR stars in this phase.

The overall goal of the project is to combine the far-infrared data with optical and sub-mm data to observationally determine the time periods of the various phases and total mass-loss associated with all galactic WR stars. In comparing our results with stellar evolution models, we hope to pin down the most likely means by which the galaxy's most massive stars evolve.

This work is supported, in part, by NASA ADP grant, NAG 5-2999.

REFERENCES

Arnal, E. M., 1992, A&A, 254, 305.

Arnal, E. M., & Mirabel, I. F., 1991, A&A, 250, 171.

Aumann, H. H., Fowler, J. W., & Melnyk, M., 1990, AJ, 99, 1674.

Cappa de Nicolau, C. E., & Niemela, V. S., 1984, AJ, 89, 1398.

Cappa de Nicolau, C. E., Niemela, V. S., & Arnal, E. M., 1986, AJ, 92, 1414.

Cappa de Nicolau, C. E., Niemela, V. S., Dubner, G. M., & Arnal, E. M., 1988, AJ, 96, 1671.

Conti, P. S., & Vacca, W. D., 1990, AJ, 100, 431.

Dopita, M. A., Bell, J. F., Chu, Y.-H., & Lozinskaya, T. A., 1994, ApJS, 93, 455.

Dubner, G. M., Niemela, V. S., & Purton, C. R., 1990, AJ, 99, 857.

Goudis, C., Meaburn, J., & Whitehead, M. J., 1988, A&A, 191, 341.

Maeder, A., & Meynet, A., 1994, A&A, 287, 803.

Manchester, R. N., & Taylor, J. H., 1981, AJ, 86, 1953.

Marston, A. P., Chu, Y.-H., & Garcia-Segura, G., 1994a, ApJS, 93, 229.

Marston, A. P., Yocum, D. R., Garcia-Segura, G., & Chu, Y.-H., 1994b, ApJS, 95, 151.

Marston, A. P., 1995a, AJ, 109, 1839.

Marston, A. P., 1995b, AJ, 109, 2257.

Marston, A. P., 1996, ApJS, submitted.

Marston, A. P., & Dickens, R. J., 1988, A&A, 193, 27.

Mathis, J. S., Cassinelli, J. P., van der Hucht, K. A., Prusti, T., Wesselius, P. R., & Williams, P. M., 1992, ApJ, 384, 197.

Miller, G., & Chu, Y.-H., 1993, ApJS, 85, 137.

Nichols-Bohlin, J. S., & Fesen, R. A., 1990, ApJ, 353, 281.

Nichols-Bohlin, J. S., & Fesen, R. A., 1993, AJ, 105, 672.

Nichols, J. S., & Fesen, R. A., 1994, A&A, 291, 283.

Niemela, V. S., & Cappa de Nicolau, C. E., 1991, AJ, 101, 572.

St.-Louis, N., & Smith, L. J., 1991, A&A, 252, 781.

Vanbeveren, D., 1988, Ap&SS, 149, 1.

Vanbeveren, D., 1994, Space Sci.Rev., 66, 327.

van der Hucht K. A., Conti, P. S., Lundstrom, I., & Stenholm, B., 1981, Space Sci.Rev., 28, 227.

van der Hucht, K., 1994, Space Sci.Rev., 66, 21.

Wood, D. O. S., & Churchwell, E., 1989, ApJ, 340, 265.

Yungelson, L. R., & Tutukov, A. V., 1991, in Wolf-Rayet Stars and Interrelations with Other Massive Stars in Galaxies, edited by K. A. van der Hucht and B. Hiddayat (Kluwer, Dordrecht), p.459.

Figure 1: The large IRAS shells observed in the IRAS Skyflux data at 60μm and 100μm (the ejecta shell around WR11 is not shown). All fields are 6° square, except where indicated on the image. In all cases the WR star is at the center of the image.

Figure 2: The variation of large IRAS shell detection rate with galactic latitude.

Figure 3: Comparison of the large IRAS shell diameters with galactic height, z.

Figure 4: The variation of local density with large IRAS shell diameter.

Figure 5: The distribution of ages of progenitor O stars associated with the large IRAS shells

.

Figure 6: Variation of shell ages with galactic height, z

Table 1

Properties of the large IRAS shells observed around WR stars

WR[2]	Type	Dist.[1] (pc)	Diam. (′)	Diam. (pc)	b[2] (°)	z[1] (pc)	Comments
2	WN2	5400	116	183	-2.41	-227.7	
3	WN3+abs	8600	60	151	-4.14	-619.9	HI shell
4	WC5	3900	120	136	-2.98	-203.0	HI shell
5	WC6	2500	81	59	-2.15	-93.8	HI shell
6	WN5	1000	171	50	-10.08	-175.1	Shell exterior to ejecta nebula S308
7	WN4	3900	35	39	-0.13	-9.1	Around NGC2359
8	WN6+WC4	3300	81	78	-3.79	-217.7	
11	WC8+O9I	300	75	6.5	-7.69	-40.1	E shell seen optically (Marston *et al.*, 1994b)
12	WN7	6300	60	111	-1.97	-216.2	
14	WC6	1800	30	16	-1.64	-51.3	Possible ejecta shell
15	WC6	1800	135	71	-1.08	-34.0	
17	WC5	3700	38	41	-3.69	-237.7	HI shell
21	WN4+O4-6	2700	110	88	-0.90	-42.4	
23	WC6	4300	30	38	-0.03	-2.5	Seen optically (Marston *et al.*, 1994a)
24	WN7+abs	2800	65	53	-1.08	-52.1	
30	WC6+abs	5700	26	43	-2.61	-260.2	Seen optically (Marston, 1995a)
31	WN4+O7	4300	34	43	0.02	1.3	
33	WC5	9200	120	323	1.9	305.0	
40	WN8	2200	180	115	-4.83	-185.4	Surrounds the ring nebula RCW58
48	WC6+O9.5I	700	133	27	-2.49	-19.1	HI shell
52	WC5	2100	1780	105	4.55	166.6	HI shell
54	WN4	6100	150	278	-2.5	-266.1	HI shell
57	WC7	4000	70	80	-5.03	-350.9	HI shell
58	WN4	4700	180	248	-3.49	-285.6	
61	WN4.5	13100	60	229	-3.91	-894.8	
66	WN8	4500	65	85	-1.83	-144.0	
68	WC7	3000	28	25	-1.88	-98.6	
69	WC9	2900	60	51	-4.82	-243.5	

Table 1 – cont.

WR[2]	Type	Distance[1] (pc)	Diam. (′)	Diam. (pc)	b[2] (°)	z[1] (pc)	Comments
70	WC8+abs	1300	170	65	-1.81	-41.2	
73	WC9	1900	110	338	3.38	619.7	
77	WC8.5	1100	32	10	-1.09	-189.1	Possible ejecta shell
82	WN8	4700	110	152	-2.32	-190.0	
85	WN6	3700	27	29	-0.61	-39.8	Seen optically (Marston, 1995a)
86	WC7+abs	1900	35	19	1.85	61.3	
87/9	WN7/WN7	1300	34	13	-0.77	-17.4	Seen optically (Marston, 1995a)
90	WC7	1300	100	38	-4.76	-108.0	HI shell
101	WN7-8	6900	80	161	-1.43	-172.6	
110	WN6	1800	30	16	0.39	12.0	Possible ejecta shell
123	WN8	6500	24	46	-4.75	-538.3	HI shell
124	WN8	3500	120	123	3.31	202.5	
132	WC6	7100	49	101	1.1	136.3	HI shell
133	WN4.5+O9.5Ia	1200	100	35	2.7	43.3	
136	WN6	1500	91	40	2.43	63.7	Surrounds the ring nebula NGC6888
139	WN5+O6	2400	142	100	1.43	60.0	
140	WC7+abs	800	110	26	4.18	58.4	HI shell
148	WN7	5200	36	54	6.47	585.7	HI shell
152	WN3	6200	21	38	-0.89	-95.6	
157	WN4.5	2300	27	18	-0.24	-9.4	
158	WN7	3900	135	154	0.1	6.8	

[1] from Conti & Vacca (1990)

[2] from van der Hucht *et al.* (1981)

Table 2: IRAS fluxes associated with 10 of the sample large rings.

WR	12μm (Jy)	25μm (Jy)	60μm (Jy)	100μm (Jy)
2	900	840	2850	3915
3	250	280	820	4320
7	15	40	490	1010
15	1520	1960	14040	44950
30	15	25	255	495
33	330	350	3125	12980
48	370	535	3720	9940
87/9	250	3245	18970	23070
133	1780	1170	12800	32000
157	120	205	1840	3790

Typical errors on observed fluxes are 20%. For WR2, numerous 12μm and 25μm point sources are in the field and the values quoted here are tentative.

Table 3: Gas masses in the large shells and derived average densities of the original insterstellar medium swept-up into the shells, made from IRAS and/or HI data.

WR	Mass $M_{\odot}$	v_{exp} (kms^{-1})	Source	Density particles cm^{-3}
2	9000		1	0.12
3	8400	10	2	0.2
5	2400	8	2	0.8
7	2200		1	2.3
15	41300		1	7.2
17	2500	8	3	3.1
30	2150		1	1.7
33	90000		1	0.22
48	1050		1	3.3
	980	9	4	3.1
52	14000	16	6	0.8
54	15000	12	6	0.05
57	32000	9	6	3.9
61	37000	20	6	0.3
87/9	2580		1	74
90	3620	10	5	5.6
123	7560	8	2	6.6
133	9000		1	13
136	8300		8	8.1
140	710	13	2	3.4
148	5700		1	2.3
	1600	6	7	0.6
157	2900		1	13

HI masses are adjusted to the object distances given by Conti & Vacca (1990). Not included are the data for the HI shells around WR125 (no IRAS shell) and WR4 and WR132 (no good estimate of shell mass available).

1 = from IRAS data presented in this paper. 2 = from Arnal (1992). 3 = from Cappa de Nicolau et al. (1986). 4 = from Cappa de Nicolau & Niemela (1984). 5 = from Cappa de Nicolau et al. (1988). 6 = from Niemela & Cappa de Nicolau (1991). 7 = from Dubner et al. (1990). 8 = from Marston (1995b).

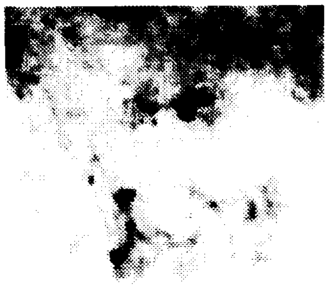

WR2 100mic

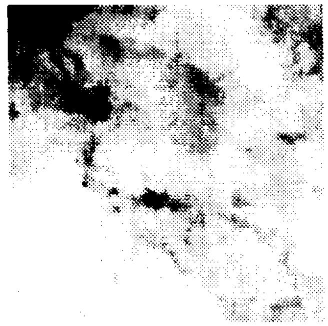

WR3 100mic

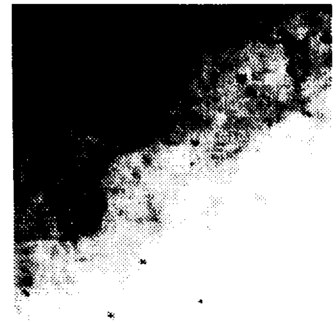

WR4 100mic

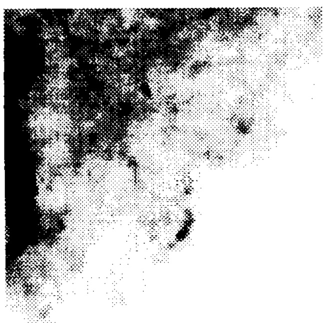

WR5 100mic

WR6 100mic

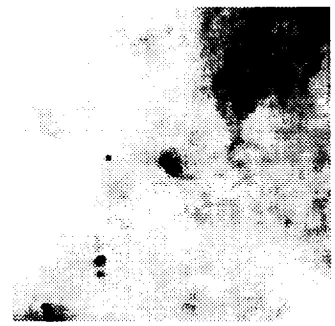

WR7 100mic

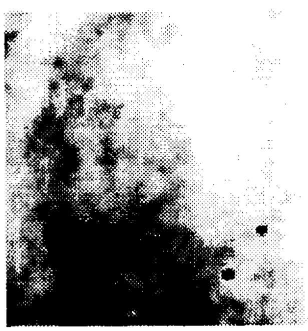

WR8 100mic

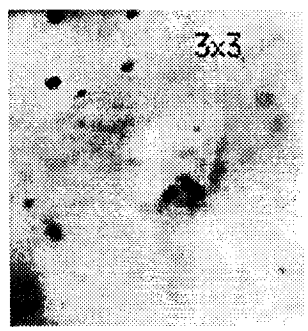

WR12 100mic

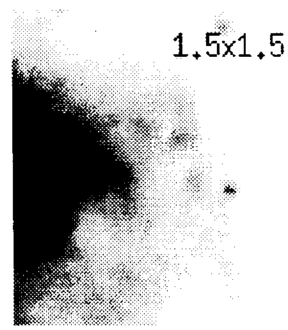

WR14 60mic

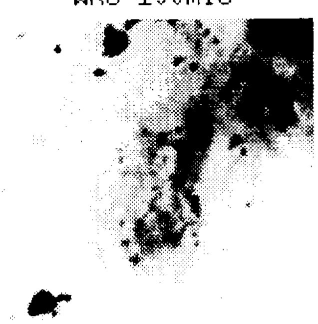

WR15 60mic

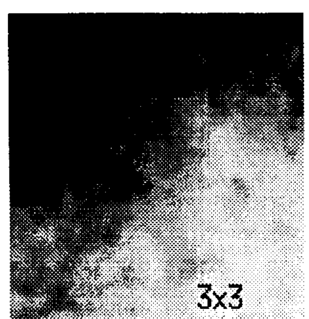

WR17 60mic

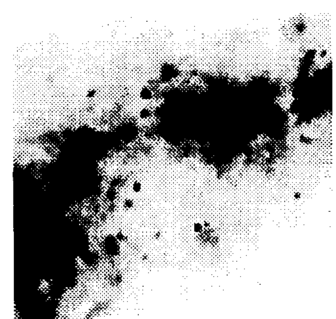

WR21 60mic

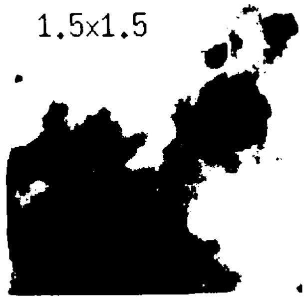

WR23 60mic

WR24 60mic

WR30 60mic

WR31 100mic

WR33 100mic

WR40 60mic

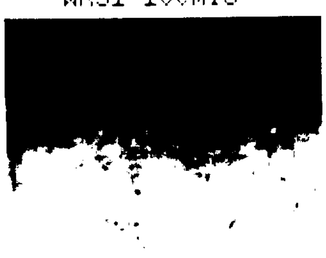

WR48 60mic

WR52 60mic

WR54 100mic

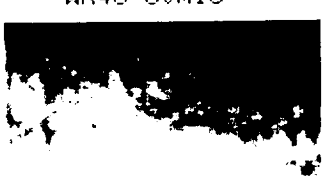

WR57 100mic

WR58 100mic

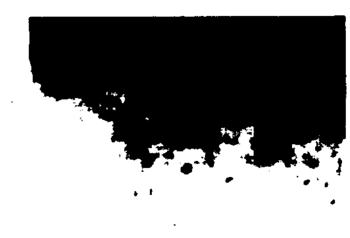

WR61 60mic

WR66 60mic

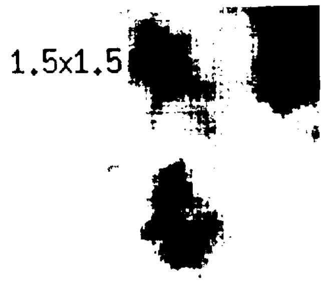

WR68 60mic

WR69 60mic

WR70 60mic

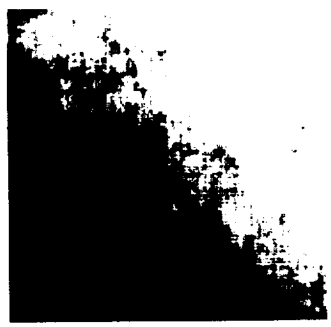

WR73 100mic

WR77 60mic

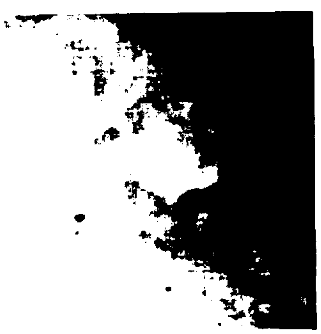

WR82 60mic

WR85 60mic

WR86 60mic

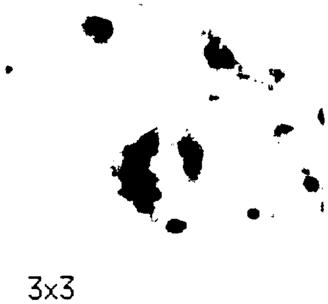

WR87/9 60mic

WR90 100mic

WR101 60mic

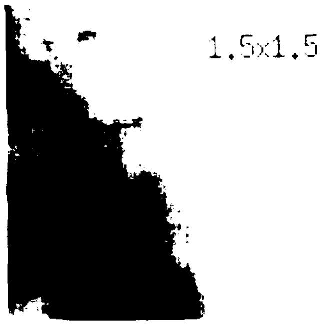

WR110 60mic


WR123 60mic


WR124 100mic

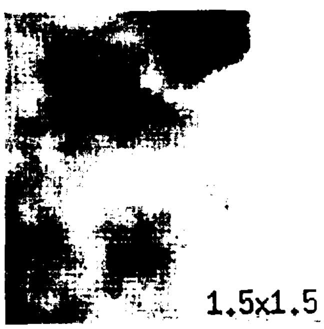

WR132 100mic


WR133 60mic

WR136 60mic


WR139 60mic


WR140 60mic

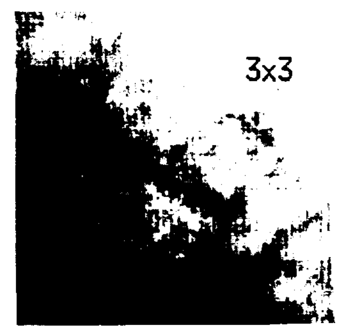

WR148 60mic

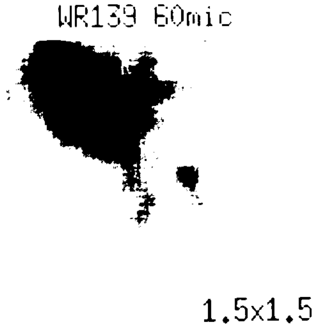

WR152 100mic

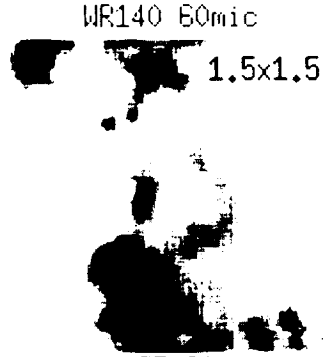

WR157 60mic

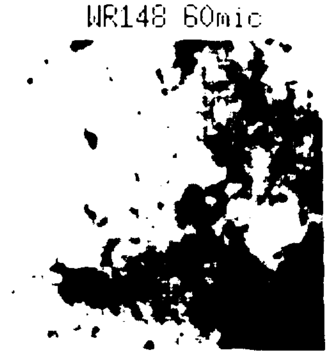
WR158 100mic

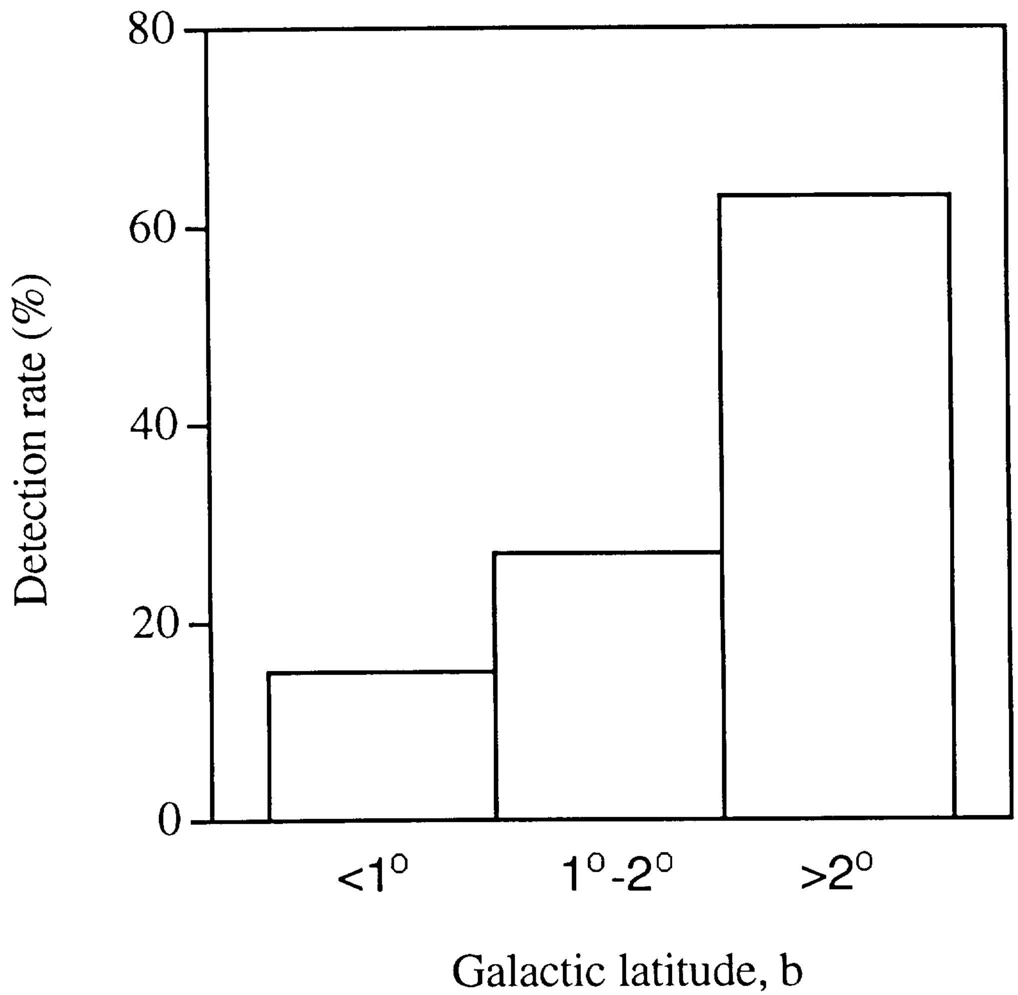
80
60
40
20
0
Detection rate (%)
<1°
1°-2°
>2°
Galactic latitude, b

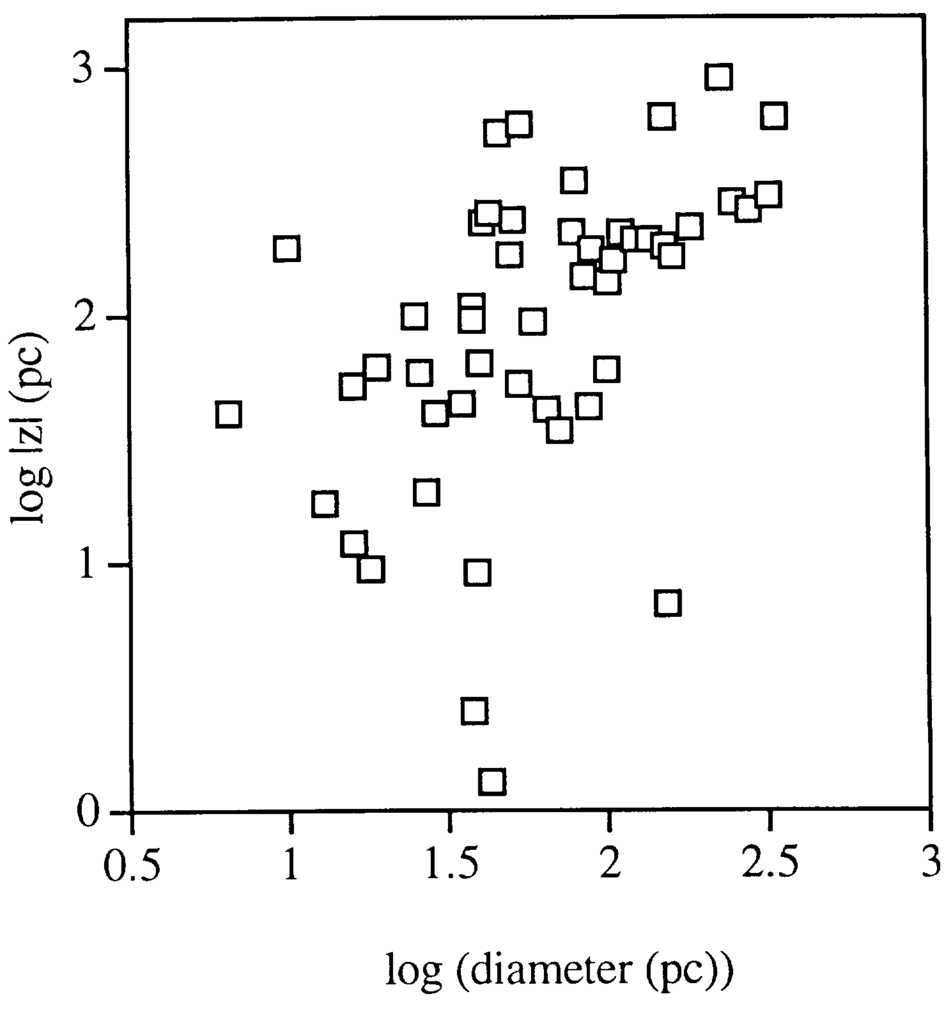
log |z| (pc)
3
2
1
0
0.5
1
1.5
2
2.5
3
log (diameter (pc))

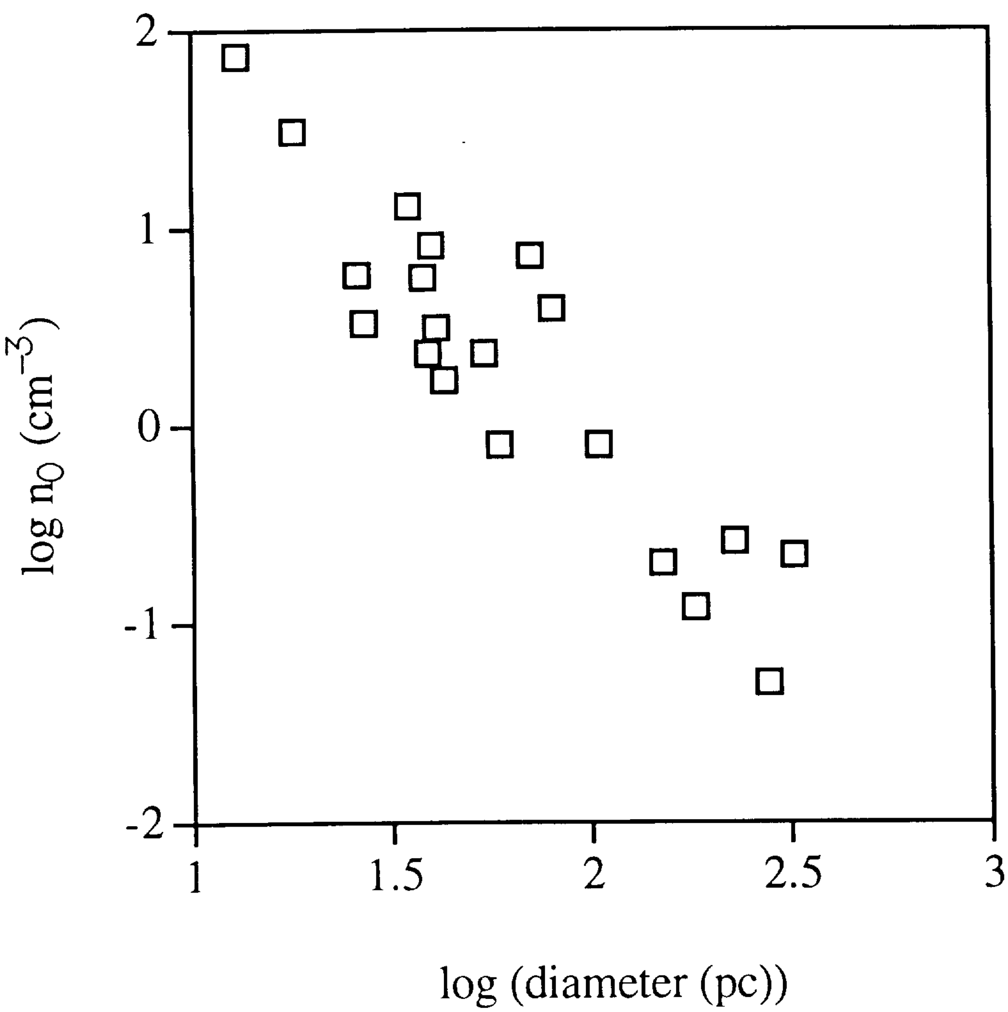

log n0 (cm-3)
2
1
0
-1
-2
1
1.5
2
2.5
3
log (diameter (pc))

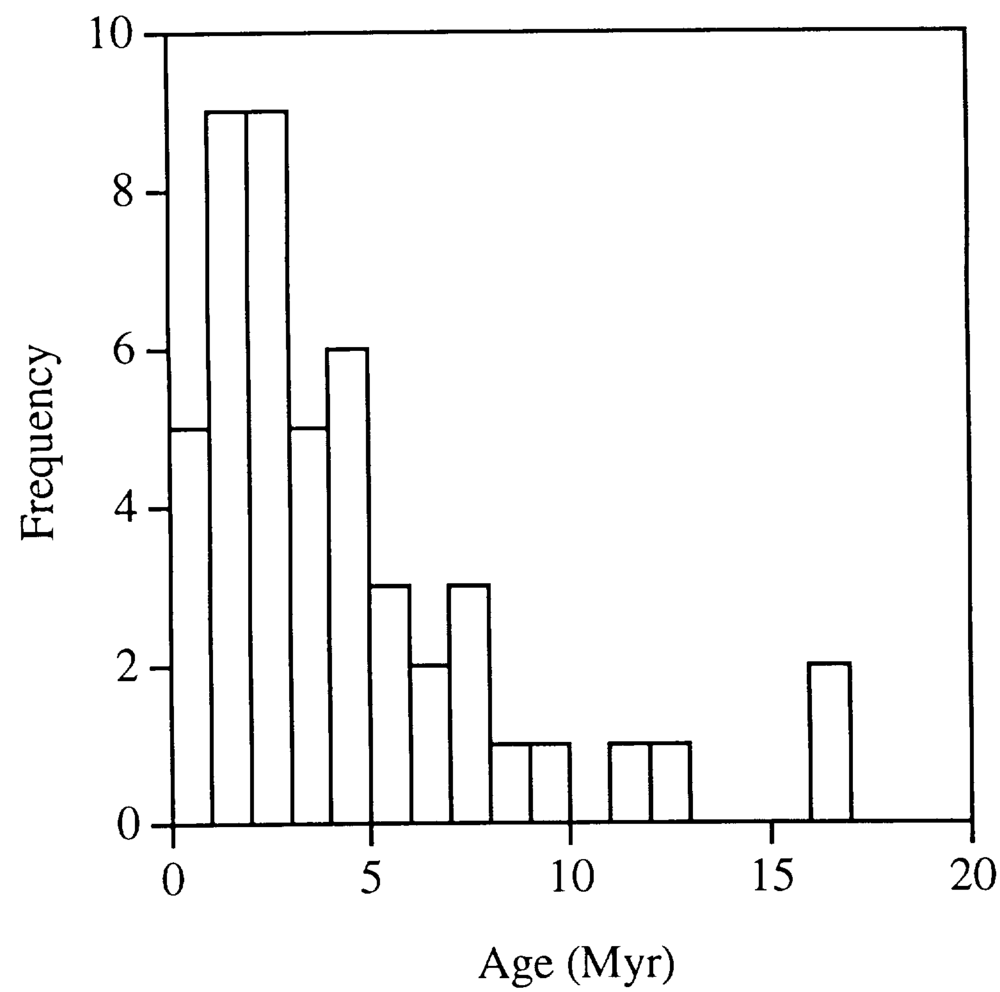

Frequency
Age (Myr)
0
2
4
6
8
10
0
5
10
15
20

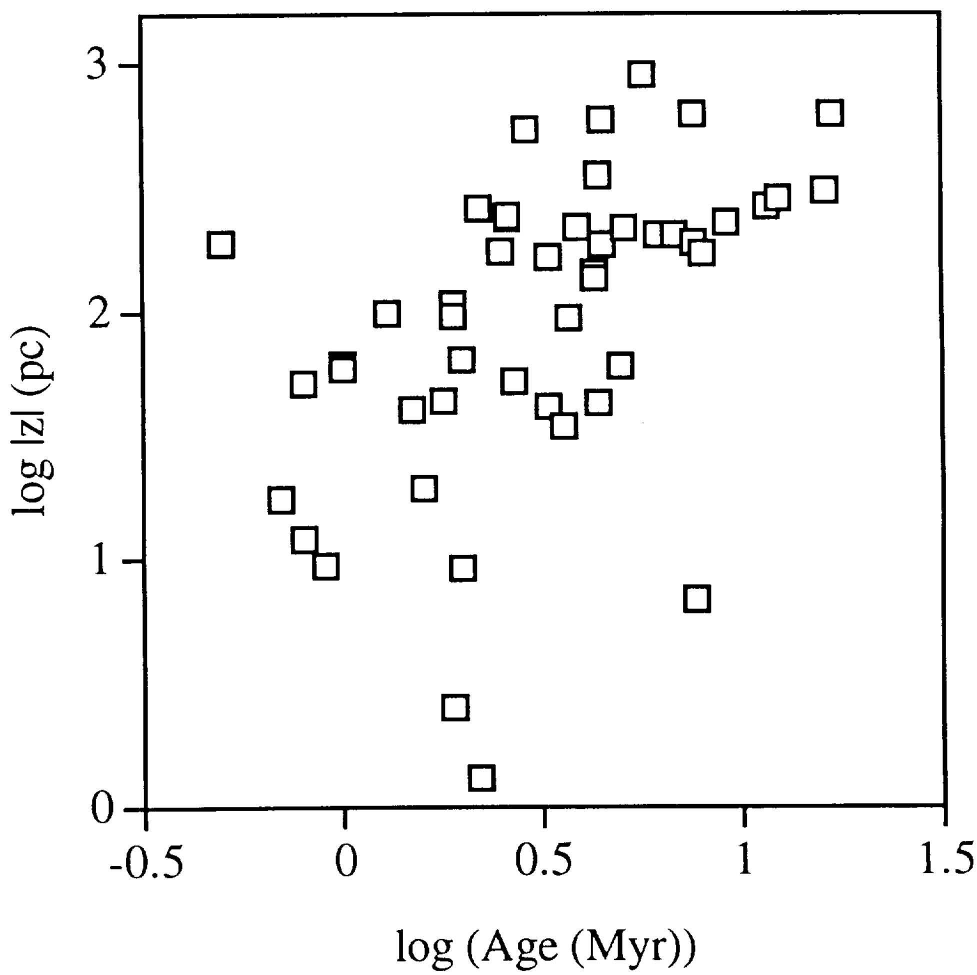

3
2
1
0
log |z| (pc)
-0.5
0
0.5
1
1.5
log (Age (Myr))